Cooperative Self-Localization of Mobile Agents

IMAN SHAMES, Student Member, IEEE
The Australian National University and National ICT Australia

BARIŞ FIDAN, Member, IEEE
University of Waterloo

BRIAN D. O. ANDERSON, Life Fellow, IEEE
The Australian National University and National ICT Australia

HATEM HMAM, Member, IEEE
Defence Science & Technology Organisation

This paper considers the problem of localizing multiple agents, e.g. unmanned aerial vehicles (UAVs), robots, etc., moving in two-dimensional space when the known data comprise 1) the inter-agent distances, and 2) the angle subtended at each agent by lines drawn from two landmarks at known positions. Later it is shown that this result has direct application in a different general robotic problem, viz. robot-to-robot relative pose determination (relative reference frame determination), using measured distances. The methods proposed are validated through simulations and experiments.

Manuscript received October 13, 2009; revised February 18 and May 17, 2010; released for publication July 8, 2010.

IEEE Log No. T-AES/47/3/941772.

Refereeing of this contribution was handled by R. Michelson.

This work is supported by NICTA, which is funded by the Australian Government as represented by the Department of Broadband, Communications and the Digital Economy and the Australian Research Council through the ICT Centre of Excellence program.

Authors' addresses: I. Shames and B. D. O. Anderson, The Australian National University and National ICT Australia, Canberra, 0200 Australia, E-mail: (iman.shames@anu.edu.au); B. Fidan, Dept. of Mechanical and Mechatronics Engineering, University of Waterloo, ON, Canada; H. Hmam, Electronic Warfare Radar Division, Defence Science & Technology Organisation, Edinburgh, Australia.

0018-9251/11/$26.00 © 2011 IEEE

I. INTRODUCTION

The problem of estimating the position of one or more mobile agents given sensed data containing some information relevant to the position is an old problem that comes in many varieties. To name a few, we can consider localization of unmanned aerial vehicles (UAVs) in open space, or localization of groups of ground mobile agents. The use of Global Positioning System (GPS) has made the task of localization easier, but still in the possible events of loss or corruption of GPS signals [1], or when the agents are operating indoors, use of GPS for localization purposes may be infeasible or limited [2].

The comprehensive study given in the Volpe report [3], prepared by the US Department of Transportation, raises awareness of the existence of GPS vulnerability abilities to several categories of signal disruptions. These can be intentional (e.g. jamming and spoofing) or unintentional (e.g. RF interference from radio, TV, cell phones and other communication transmitters). The main findings of the report are that vulnerability abilities, which range from momentary to severe, affect all transportation modes and related infrastructure. The report also emphasizes that such vulnerabilities can be mitigated by awareness, planning, or using independent backup systems and/or alternate procedures in safety-critical applications [3]. A comprehensive analysis of backup navigation systems is beyond the scope of this paper but includes long range navigation (LORAN) systems and inertial navigation systems (INS). In this paper we address the navigation problem where self-localization is achieved cooperatively among a team of distance sensing agents.

The first problem that we consider in this paper has arisen in the context of small groups of agents sensing the angle subtended at each of them by two landmarks at known positions. This problem originated from flight trials with real UAVs conducted by the Defence Science & Technology Organisation (DSTO) of Australia. Loss or corruption of GPS signal is a reality, and a method was needed to localize the formation in such situations. The position information of the two landmarks is available, as are inter-agent distances. The problem considered here is very similar to the problems considered in [4]–[10]. While the solution of the problems treated in the above references need at least three landmarks, in this paper we consider initially having access to only two. In order to provide enough information to compensate for the lack of information about a third landmark, a cooperative localization scheme is considered. Cooperative localization is achieved by the agents using distance measurements to other agents.

The first arrangement, on which the later developments are based, that we consider is depicted in Fig. 1(a), n mobile agents (in this case $n = 3$),

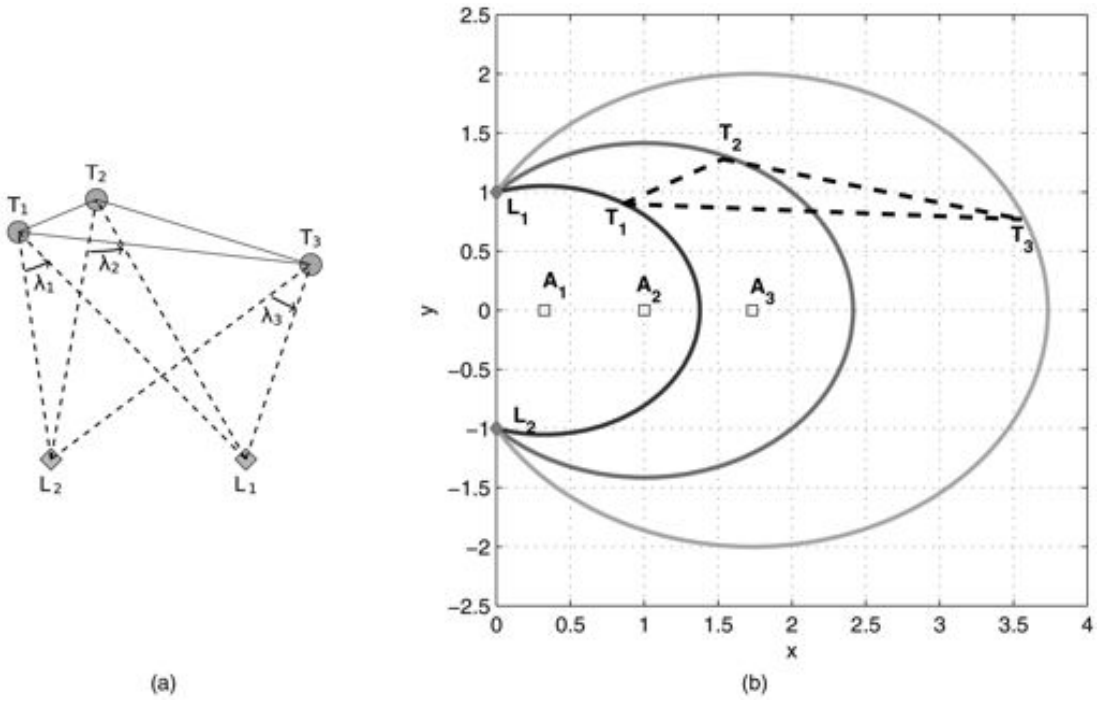

Fig. 1. (a) Arrangement we consider in this paper. (b) Loci of agents T_i, $i = 1,2,3$, for $\angle L_1 T_i L_2 = \lambda_i$, and L_1 and L_2 are landmarks with known positions. Solid lines construct the four-bar linkage mechanism with the coupler point. Note that loci are NOT full circles, but only arcs.

designated T_1, T_2 and T_3 are to be localized; the inter-agent distances are known. Additionally, the agents detect two landmarks located at positions L_1 and L_2, which are known to the agents. The landmarks can be radars, RF beacons or some visible features if an imaging sensor is used. Each agent collects the bearing angle information to each of the landmarks. However, with no GPS information, there is no absolute heading reference for each agent, and the bearing angle information cannot be used directly for localization purposes. However, using the angle difference the need for knowing the heading is removed. This angle difference is the angle subtended at each agent by the two landmarks (λ_i, $i = 1,2,3$), see Fig. 1(a), and it can therefore be concluded that each agent i is located on a circle of known centre A_i and radius R_i (determined by λ_i) and passing through the two landmarks. The centres, A_i ($i = 1,2,3$) lie on the perpendicular bisector of the line joining the two landmarks. A priori information is assumed to be available which positions all agents on the same known side of the line joining the two landmarks.

The cooperative localization task is then to put the pieces of information together, i.e., inter-agent distances, subtended angles and landmark positions, and localize the agents. Note here that the localization is to be achieved instantaneously; we are not envisaging collecting information from agents at a number of successive instants of time and using them to infer position at a single instant of time (the connection with Kalman filtering is explored further below). In distance-based localization literature the nodes with known position are called anchors (beacons) [11], and since each A_i is determined exactly, they can be considered as anchors as well. Due to the nature of the problem mentioned above these anchors are collinear. However, the results obtained in this paper are not limited to collinear anchors, and can be applied to scenarios with arbitrary arrangement of the anchors. Note also that we later extend the results to systems with more than three agents capable of measuring the subtended angle by the landmarks.

It is shown in Section IV that the solution count for the above localization problem (involving three agents) is less than 12. If there is no unique solution, what is the point of this analysis? There are in fact several ways in which it can be relevant. First, GPS data may be intermittently available to an agent. When it is available, localization is obviously unique. When it ceases to be available, the fact that the agents are moving continuously with their initial position known means that there will be a basis for making the correct selection out of a finite number of localization possibilities at subsequent times.[1] Second, given that the number of possible solutions to the localization problem is finite, it may be that additional very crude data indeed (e.g. agent T' is located in this general

[1]At least until the agents move to positions corresponding to a double solution of the localization problem, after which two tracks would have to be followed assuming no disambiguating information.

region) will be enough to disambiguate the multiple solutions. Third, if more agents are available, then the additional information will generically allow unique localization, and indeed, when measurements are noisy, will in general allow some amelioration of the distorting effects of the noisy measurements. Lastly, the method proposed in this paper can be considered as batch processing of the agent locations serving to initialize and improve the updates of a Kalman-based filter which tracks the agent positions as the agents move in their environment. Kalman-based filters are also prone to errors when the agent's motion model deviate significantly from the actual agent motion. Our batch processing method can guard against such behavior and reinitialize the filter.

There is a vast body of literature using Bayesian methods that deals with localization problems. For example, in [12] a collective localization problem based on Kalman filtering is proposed, and [13] uses a Gaussian sum filter to solve the initialization problem in bearing only simultaneous localization and mapping (SLAM). Differently from these approaches, the tools for obtaining our results are drawn from two nonconventional sources. The first is the theory of rigid graphs, see e.g. [14]–[17]. In recent years, its relevance to localization of sensor networks has come into prominence [11, 18]. A good deal of the theory of rigid graphs deals with the question of when localization is possible [19, 20]. The second source we draw on is the mechanical engineering literature dealing with four-bar linkage mechanisms [21, 22]. As it turns out, this literature has developed ideas for describing the loci of points that are part of a planar mechanism made up from pin joints and rigid bars that provide distance constraints between the joints.

The method developed here can be used to calculate multiple localization solutions in other scenarios, such as localization of mobile wireless sensor networks, as well. For instance one can solve a more general form of the problem studied in [23] with the methods introduced here. We apply the method to a second problem involving robot-to-robot reference frame determination. This problem first appeared in [24], [25], and although the practical origins of the problems are different, the mathematical essence is the same as the one considered here. The problem considered in [24], [25] is how to determine the relative pose of a pair of robots that move on a plane while measuring the distance to each other, and what the possible solutions for different numbers of inter-robot distance measurements are. Another recent set of studies related to this problem addresses frame localization in a wireless network, where the goal is to find the reference frame orientation of the nodes in a network with respect to a reference node using bearing measurements only. For further information see [26], [27]. In later sections of this paper, we present the application of our localization results to robot-to-robot relative reference frame determination in two-dimensional space using range measurements, introduce a numerical method for identifying those agent settings that are sensitive to the measurement noise, and propose algorithms for dealing with measurement errors.

Note that a subset of our studies on the first problem with only three agents have already been presented in [28]. However, in this paper in addition to mathematically proving the results presented in [28], we extend the results to systems with more than three agents capable of measuring the subtended angle by the landmarks. Moreover, we propose algorithms for dealing with measurement errors and test them via real robot experiments in addition to numerical simulations.

The paper is organized as follows. Section II reviews basic material on rigid formations and sensor network/formation localization. Section III formally describes and analyses the main problem described in the beginning of this section using the tools introduced in Section II. This analysis enables us to argue immediately that the localization problem generically has more than one solution. In Section IV, we review the results in the mechanical engineering literature regarding four-bar linkage mechanisms and application of these results to the localization problem defined in Section II. In Section V, we consider the cases where some extra information about other agent(s) and/or other landmark(s) is available. In Section VI, we address robot-to-robot relative reference frame determination problem. In Section VII, we present a geometric sensitivity analysis for different positions of the agents. In Section VIII, we propose a method to deal with measurement noise. In Section IX, we illustrate the results with some numerical examples and set up two experiments to test the method for solving robot-to-robot reference frame determination. Section X contains concluding remarks.

II. RIGID FORMATIONS AND LOCALIZATION

In this section, we review some aspects of the problem of localizing, i.e., determining the positions of agents in a formation where a number of inter-agent distances are known, and also some absolute position data is available. We draw on literature on rigid graph theory and its application to sensor network localization [11, 18–20].

A formation of point agents in the plane, $\mathcal{F}$, can be represented by a graph $\mathcal{G}(\mathcal{V},\mathcal{E})$, with vertex set $\mathcal{V}$ and edge set $\mathcal{E}$, where the vertices in $\mathcal{V}$ correspond to the agents, and there is an edge in the graph between two vertices $v_1, v_2 \in \mathcal{V}$ just when the distance between the corresponding agents of the formation is known. We call $\mathcal{G}$ the underlying graph of $\mathcal{F}$.

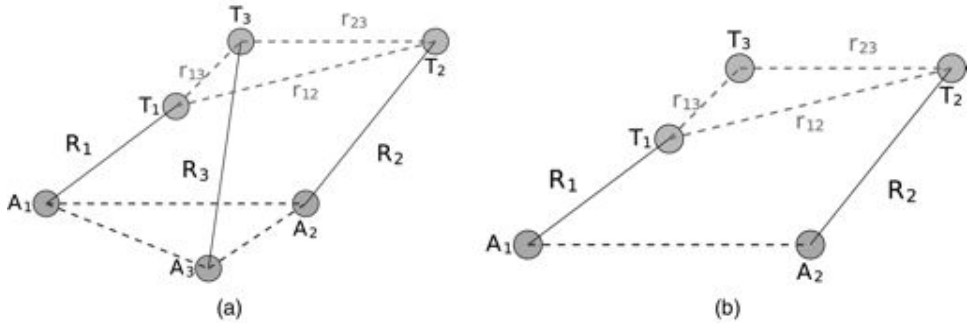

Fig. 2. (a) Graph described in Problem 1. (b) Four-bar linkage mechanism obtained after deletion of A_3T_3.

Assigning coordinate values to each vertex of a graph, $\mathcal{G}(\mathcal{V},\mathcal{E})$, so that the Euclidean distance between any two adjacent vertices is equal to the edge length associated with the edge joining these two vertices, is the graph realization problem. Given one solution to the graph realization problem, it is trivial that any translation, rotation, or reflection of this solution is another solution. All solutions of this sort are congruent. So it is also relevant to ask whether there can be two solutions which are not congruent, and whether, disallowing translations, rotations, or reflections, the number of distinct solutions is finite or infinite. When there can only be one family of congruent solutions, we say that the graph realization problem has a unique solution.

Hendrickson in [19] presents necessary conditions for a graph to be uniquely realizable in $\mathbb{R}^2$, i.e., with one family of congruent solutions, and the conditions were proved later by Jackson and Jordan [20], to be necessary and sufficient.

These conditions involve two concepts, namely redundant rigidity of a graph, and three-connectedness of a graph. The concept of redundant rigidity requires a prior concept of rigidity. A formation $\mathcal{F}$ is called rigid if by explicitly maintaining distances between all the pairs of agents whose representative vertices are connected by an edge in $\mathcal{E}$, the distances between all other pairs of agents in $\mathcal{F}$ are consequentially held fixed as well. The reader may refer to [14]–[16] for detailed information on rigid formations and rigidity.

A redundantly rigid formation is one which remains rigid when any single edge constraint is removed. By contrast, as we shall use the concept in the next section, a minimally rigid formation is one which ceases to be rigid when any single edge constraint is removed. The underlying graph of a formation is called rigid, redundantly rigid, and minimally rigid if the formation is, respectively, rigid, redundantly rigid, and minimally rigid.

The notion $\mathcal{G}$ of a 3-connected graph is standard, see [29]. Such a graph has the property that between any two vertices, three nonintersecting paths can be found.

Jackson and Jordan's result [20] is as follows

THEOREM 1 *Consider a two-dimensional formation $\mathcal{F}$ with underlying graph $\mathcal{G} = (\mathcal{V},\mathcal{E})$. Then the graph realization problem is uniquely solvable for generic values of the formation edge lengths (inter-agent distances) if and only if $\mathcal{G}$ is redundantly rigid and 3-connected.*

A graph $\mathcal{G}$ with the two properties in Theorem 1, i.e., redundant rigidity and 3-connectedness is termed globally rigid. For a formation which is rigid but not globally rigid, at least one of the two ambiguities known as flip ambiguity or discontinuous flex ambiguity occurs [19]. The reader may refer to [16], [19] and references therein for further information on these ambiguities.

III. THE FORMATION LOCALIZATION PROBLEM

In this section, we consider a formation with a particular structure and show that it is minimally rigid. Accordingly, even with the knowledge of three agent positions, this formation will not be uniquely localizable. We later relate this formation and the associated result to the localization problem presented in the Introduction. The problem of this section is formulated as follows.

PROBLEM 1 *Consider a formation $\mathcal{F}$ with the underlying graph $\mathcal{G}(\mathcal{V},\mathcal{E})$, where $\mathcal{V} = \mathcal{T} \cup \mathcal{A}$ is the set of vertices with $\mathcal{T} = \{T_1,T_2,T_3\}$, $\mathcal{A} = \{A_1,A_2,A_3\}$. The agents in $\mathcal{A}$ are known as anchor agents, and those in $\mathcal{T}$ as target agents. Furthermore, $\mathcal{E} = \{T_1T_2,T_1T_3,T_2T_3,A_1A_2,A_1A_3,A_2A_3,A_1T_1,A_2T_2,A_3T_3\}$ is the set of edges. Knowing the length of all edges in $\mathcal{E}$, and the exact positions of the anchor agents:*

a) Can one localize the target agents, uniquely, or to one of a finite number of sets of positions?

b) If so, what are the possible localization solutions?

An example of the formation $\mathcal{F}$ described in Problem 1 is depicted in Fig. 2(a). A crucial fact pertinent to answering the localization problem is that the formation described in Problem 1, is a minimally rigid formation. Two ways are presented in the following paragraphs to see this fact.

LAMAN'S THEOREM [14] *Laman's Theorem provides a combinatorial way to check rigidity, and minimal rigidity. It requires the idea of an induced subgraph of a graph $\mathcal{G} = (\mathcal{V}, \mathcal{E})$. Let $\mathcal{V}'$ be a subset of $\mathcal{V}$. Then the subgraph of $\mathcal{G}$ induced by $\mathcal{V}'$ is the graph $\mathcal{G}' = (\mathcal{V}', \mathcal{E}')$ where $\mathcal{E}'$ includes all those edges of $\mathcal{E}$ which are incident on a vertex pair in $\mathcal{V}'$.*

THEOREM 2 (Laman's Theorem [14]) *A graph $\mathcal{G} = (\mathcal{V}, \mathcal{E})$ in $\mathbb{R}^2$ of $|\mathcal{V}|$ vertices and $|\mathcal{E}|$ edges is rigid if and only if there exists a subgraph $\mathcal{G}' = (\mathcal{V}, \mathcal{E}')$ with $2|\mathcal{V}| - 3$ edges such that for any subset $\mathcal{V}''$ of $\mathcal{V}$, the induced subgraph $\mathcal{G}'' = (\mathcal{V}'', \mathcal{E}'')$ of $\mathcal{G}'$ obeys $|\mathcal{E}''| \leq 2|\mathcal{V}''| - 3$. It is minimally rigid if $|\mathcal{E}| = 2|\mathcal{V}| - 3$.*

It is easy to check for the graph of Fig. 2(a) that $|\mathcal{E}| = 2|\mathcal{V}| - 3$; one takes $\mathcal{G}' = \mathcal{G}$ and can verify the counting condition for all induced subgraphs.

Combination of Rigid Formations [17]: Another way of proving minimal rigidity of a formation is by showing that it is a certain type of combination of two minimally rigid formations. The key theorem is as follows.

THEOREM 3 ([17]) *Let $\mathcal{F}_1$ and $\mathcal{F}_2$ be two rigid formations, and consider a formation $\mathcal{F}$ formed by connecting these two formations with three edges, each edge incident on one vertex of $\mathcal{F}_1$ and one of $\mathcal{F}_2$, with no two edges incident on the same vertex. Then $\mathcal{F}$ is rigid. Moreover, if $\mathcal{F}_1$ and $\mathcal{F}_2$ are minimally rigid, so is $\mathcal{F}$.*

Observe that a triangle is obviously minimally rigid. The theorem then applies identifying $\mathcal{F}_1$ with the triangle formed by A_1, A_2, and A_3 and $\mathcal{F}_2$ with the triangle formed by T_1, T_2, and T_3. In the light of the minimal rigidity of the formation of Fig. 2(a), there will be noncongruent formations meeting the distance constraints. Then, even though the positions of A_1, A_2, and A_3 are fixed, the positions of T_1, T_2, and T_3 will not be uniquely determinable.

We now explain how the problem posed in the Introduction fits into the framework we have just described.

It has been assumed that the agents form a triangular formation, where T_i is the ith agent with $[x_{T_i}, y_{T_i}]^\top \in \mathbb{R}^2$ as its coordinates. The separation distance between two agents i and j is known and equal to r_{ij} (or r_{ji}). For a given agent T_i, and two landmarks with known position L_1 and L_2, the locus for the position of T_i when $\angle L_1 T_i L_2 = \lambda_i$, is a part of a circle denoted by $C(A_i, R_i)$ where $R_i = d/2\sin(\lambda_i)$ is the radius of the circle and A_i is the center. Furthermore, assuming that the origin of the global coordinates frame is the middle of L_1L_2, $d = \overline{L_1L_2}$ and the x-axis coincides with the perpendicular bisector of L_1L_2 the position of A_i is considered to be $[x_i, y_i]^\top = [d/(2\tan\lambda_i), 0]^\top$. Note that T_i, L_1 and L_2 lie on the same circle described above.

In Fig. 1(b) each mobile platform T_i, $i = 1,2,3$, and the associated circles are depicted. In this case the centres of the circles A_i serve as the virtual anchors, since we know their exact positions in the plane. Hence, the agents T_i ($i \in \{1,2,3\}$) in the formation and these virtual anchors A_j ($j \in \{1,2,3\}$) form a graph which satisfies the conditions presented in Problem 1. Here using the concept of four-bar linkage mechanism, which is discussed in the next section, an upper bound for the number of localization possibilities is presented.

IV. FOUR-BAR LINKAGE MECHANISMS AND APPLICATION TO THE LOCALIZATION PROBLEM

In a four-bar linkages mechanism, the fixed link is called the frame. The two side links that can revolve around the ends of the frame are called side links, and the remaining (fourth) link is called the coupler.

If in Fig. 2(a), we delete the edge connecting A_3 to T_3, $A_1A_2T_1T_2$ can be considered as a four-bar linkage mechanism (see Fig. 2(b)). In this mechanism, T_3 is termed the coupler point. The curve that this coupler point moves on in both open and cross configurations is called the coupler curve. Generally coupler curves are closed curves, but for some special mechanisms we will have open coupler curves, These correspond to situations where the area enclosed by the coupler curve shrinks to zero.

A coupler curve K_C may comprise either a single part or a bipartite curve (a bipartite curve is one with two branches, like a hyperbola.). In the case that K_C is bipartite we denote the branches as K_{C_1} and K_{C_2}, where K_{C_1} is the curve obtained by the coupler point in open configuration and K_{C_2} is constructed by the curve in cross configuration.

For a given four-bar linkage mechanism, in Fig. 2(b), the equation of the coupler curve (bipartite or single part) K_C when the center of Cartesian coordinates system is placed on A_1, and A_1 and A_2 are placed on the x-axis, is [21]

$$\begin{aligned} & r_{23}^2((x_{T_3}-k)^2 + y_{T_3}^2)(x_{T_3}^2 + y_{T_3}^2 + r_{13}^2 - R_1^2)^2 - 2r_{23}r_{13} \\ & \quad \times ((x_{T_3}^2 + y_{T_3}^2 - kx_{T_3})\cos\eta_3 + ky\sin\eta_3) \\ & \quad \times (x_{T_3}^2 + y_{T_3}^2 + r_{13}^2 - R_1^2) + ((x_{T_3}-k)^2 + y_{T_3}^2 + r_{23}^2 - R_2^2) \\ & \quad + r_{13}^2(x_{T_3}^2 + y_{T_3}^2)((x_{T_3}-k)^2 + y_{T_3}^2 + r_{23}^2 - R_2^2)^2 \\ & \quad - 4r_{23}^2r_{13}^2((x_{T_3}^2 + y_{T_3}^2 - kx_{T_3})\sin\eta_3 - ky_{T_3}\cos\eta_3)^2 = 0 \end{aligned} \tag{1}$$

where k is the length of the frame link, $\overline{A_1A_2}$, and $\eta_3 = \angle T_1T_3T_2$.

In addition another coupler curve K_C' can be obtained from the reflection of K_C, when A_1A_2 is the image axis. In general the equation describing K_C' can be obtained by substituting $-y$ for y in (1). In the case of a bipartite K_C we denote the branches of K_C' as K_{C_1}'

and K'_{C_2}. As a result the locus of the coupler point is made up of two polynomial curves each with degree of six.

1) *Application to The Formation Localization Problem*: From our analysis of Problem 1 we know that T_3 is placed on a circle with A_3 as its center and R_1 as its radius. So the possible solutions for the localization problem can be obtained from the calculation of intersections of the circle $C(A_3,R_3)$ and the two coupler curves. One might then expect that for each coupler curve we would have 12 intersection points (real and complex), and as a result 24 localization solutions in all. Somewhat surprisingly perhaps, the following theorem states that the maximum number of localization solutions is 12.

But first we note that in [22, sec. 3] the number of intersections of coupler curves and a circle is computed using concepts of circularity and order of the curves. From [22], see main formula (3), we have the following lemma.

LEMMA 1 *The circle $C(A_3,R_3)$ and the coupler curve described by* (1) *has at least two and at most six real points of intersection.*

THEOREM 4 *The maximum number of (real) localization solutions for Problem 1 is 12. For generic values of distances and angles, the minimum number of localization solutions is 4.*

PROOF Equation (1) corresponds to the coupler curves for the four-bar linkages mechanism depicted in Fig. 2(b) corresponding to Problem 1 [21]. Since there are 2 (single part or bipartite) coupler curves (the second one is the image of the first one when the frame link is the image axis) and for each coupler curve based on Lemma 1, there are a maximum of 6 and a minimum of 2 possible solutions, we have at most 12 possible solutions, and at least 4 localization solutions.

Returning to the problem presented in Section I, based on the procedure introduced earlier in this section for constructing a four-bar mechanism by deleting edge A_3T_3, we can have the linkage mechanism depicted by solid lines in Fig. 1(b). In addition, here for the coupler curve equation we have, $k = (d/(2\tan\lambda_2)) - d/((2\tan\lambda_1))$, $R_1 = d/(2\sin\lambda_1)$, and $R_2 = d/(2\sin\lambda_2)$. From Theorem 4 we can have up to 12 localization solutions.

REMARK 1 Terming intersection points that occur on that part of the circle for which the angle subtended by the landmarks does not equal the measured value for the angle, i.e., the undrawn shorter arcs joining L_1L_2 in Fig. 1(b), as invalid solutions, for some cases where there are 4 intersections and the two of the intersection points are invalid solutions, there are only 2 (mirror image) localization solutions.

REMARK 2 For generic values of distance and angles the number of solutions for Problem 1 can be 4, 8, or 12. These counts include the repeated cases as well.

REMARK 3 Theorem 4 holds for the cases that the distance and angle information can be associated with a real scenario. For instance for the cases that inter-agent distances are not feasible to construct a triangle, seeking a localization solution is irrelevant.

B. Localization of Larger Formations

The following theorem extends the current idea of localization of three agents to localization of a formation with a globally rigid underlying graph.

THEOREM 5 *Consider a formation $\mathcal{F}$ with the underlying globally rigid graph $\mathcal{G}(\mathcal{V},\mathcal{E})$, and the three agents, T_1, T_2, and T_3 in the formation which form a triangle. Assuming that these three agents are the only agents capable of measuring the angle subtended at them by the two landmarks L_1 and L_2, with known positions, then there are at most twelve possible localization solutions for the formation.*

PROOF Theorem 4 states that the upper bound for the number of localization solutions of a triangular formation using the value of the angles subtended at each agent by two landmarks is 12. On the other hand, in [20] it has been shown that the necessary and sufficient condition for unique localization of a formation is that the associated graph is globally rigid and there are 3 nodes with exactly known positions. As a result, for each possible localization of three agents there is a localization solution for the whole formation, so there are up to 12 possible localization possibilities for the formation.

C. A Localization Algorithm

We conclude this section by providing the following localization algorithm to address Problem 1(b). The algorithm provided here can be used to find up to six localization solutions; for finding the rest one can mirror the solutions with respect to the line connecting A_1 to A_2.

ALGORITHM 1 *3 Agent and 2 Landmark Localization*

Find $m \leq 6$ real intersection points of (1) *and* $(x-x_3)^2 + (y-y_3)^2 - R_3^2$, $T_{3i} = [x_{iT_3}, y_{iT_3}]^\top$, $i = 1,\ldots,m$.
for $i = 1$ *to* m **do**

Solve the system of equation for x_{iT_1}, y_{iT_1}, x_{iT_2}, and y_{iT_2}:

$$(x_{iT_3} - x_{iT_1})^2 + (y_{iT_3} - y_{iT_1})^2 - r_{13}^2 = 0$$

$$(x_{iT_3} - x_{iT_2})^2 + (y_{iT_3} - y_{iT_2})^2 - r_{23}^2 = 0$$

$$(x_{iT_2} - x_{iT_1})^2 + (y_{iT_2} - y_{iT_1})^2 - r_{12}^2 = 0$$

$$(x_1 - x_{iT_1})^2 + (y_1 - y_{iT_1})^2 - R_1^2 = 0$$

$$(x_2 - x_{iT_2})^2 + (y_2 - y_{iT_2})^2 - R_2^2 = 0$$

$S_i = [x_{iT_1}, y_{iT_1}, x_{iT_2}, y_{iT_2}, x_{iT_3}, y_{iT_3}]$
endfor
Return S as the set of m localization solutions.

V. THE EFFECT OF HAVING EXTRA LANDMARKS AND/OR AGENTS CAPABLE OF MEASURING ANGLES

In this section we consider that some extra information about another agent and/or another landmark is available. In the first subsection we consider the effect of having extra landmarks, and in the second one we consider the situation where there are more agents in the formation that are capable of measuring the angle subtended at itself by the two landmarks.

A. Extra Landmarks

Suppose another landmark L_3 is positioned at a known position in the plane, and further imagine that agent T_1 can measure the subtended angle by landmarks L_1 and L_2, L_1 and L_3, and L_2 and L_3. These three angle measurements result in having three circles with the common point of intersection exactly at T_1 for generic positions for T_1. Hence, having another landmark generically disambiguates the multiple localization solutions.

There are some certain geometries for which a unique solution for the agent cannot be calculated, for instance, if the agent is located on the circumcircle of the triangle $\triangle L_1L_2L_3$, one cannot localize it.

B. Extra Agents Capable of Measuring Angles

Now assume that we have another agent T_4 that can measure its distance from agents T_1, T_2, and T_3. Furthermore, it can measure the angle subtended at itself by the two landmarks λ_4. Knowing this angle we can characterize another anchor node, A_4 with known position, similar to A_1, A_2, and A_3. Additionally, we know the distance between T_4 and A_4. A_i, $i = 1,\dots,4$, form a complete (and therefore globally rigid) graph and we already have implicitly assumed that T_1, T_2, T_3, and T_4 also form a complete graph. We know from [30] that by connecting a globally rigid graph to another one using four edges the resulting graph is globally rigid as well, and as a result, for generic positions of the agents has a unique realization. So the formation described above has a unique localization solution for generic positions of agents and landmarks, and again addition of an agent capable of measuring the angle subtended at itself by the two landmarks disambiguates the multiple localization solutions. The crucial point here is that the anchor nodes A_1, A_2, A_3, and A_4 are collinear, which violates genericity. This collinearity results in having mirror localization solutions at different sides of the line that the anchors are placed on. The following theorem formally establishes the effect of collinearity on the localization in this scenario.

THEOREM 6 *The possible number of localization solutions for a formation as described above is two, where each solution is the mirror image of the other one when A_1A_2 is the mirror axis.*

PROOF See Appendix I.

VI. RELATIVE REFERENCE FRAME DETERMINATION

In this section we consider the problem of determining the rotation and translation associating the relative reference frames of a pair of robots where the robots can measure their distance from each other. In [25] the problem of determining the relative reference frames of a pair of robots that move on a plane while measuring distance to each other is studied. In what comes next we state this problem.

PROBLEM 2 *Consider two agents (robots) A_1 and A_2 in $\mathbb{R}^2$, whose initial reference frames are indicated by Σ_1 and Σ_2, respectively. The two agents move through a sequence of n unknown different positions with a reference frame associated with each position, $\Sigma_1,\Sigma_3,\dots,\Sigma_{2n-1}$ for A_1 and $\Sigma_2,\Sigma_4,\dots,\Sigma_{2n}$ for A_2, where $n \in \mathbb{Z}$. Their inter-agent distance, $d_{i,i+1}$ is measured at each of these positions, where $i \in \{1,3,\dots,2n-1\}$. In addition each agent is capable of estimating its current reference frame orientation and displacement with respect to its initial reference frame using dead-reckoning (odometry). In other words A_1 and A_2 estimate the position vectors $p^1_3,\dots,p^1_{2n-1}$ and $p^2_4,\dots,p^2_{2n}$ respectively. Additionally they know the rotation matrices that relate the orientations of their initial reference frame and all the others in their own sequence, e.g. R^1_3 is the rotation matrix relating Σ_1 to Σ_3. The task is to find p^1_2 and R^1_2 using this information.*

First, assume that the origins of the reference frames of the agents at each time are the vertices of a graph, and if the distance between any pair of the origins is known there is an edge connecting them together; see Fig. 3(a). We call the resulting graph G_{a-a}. Without loss of generality we select Σ_1 as our reference frame for solving the problem. As a result of this selection, the origins of the reference frames $\Sigma_1,\Sigma_3,\dots,\Sigma_{2n-1}$ can be calculated and they can be considered as anchor points for the formation with G_{a-a} as its underlying graph (In addition the rotation matrix relating each of them to Σ_1 can be calculated as well.). The goal here is to find the positions of the origins of $\Sigma_2,\Sigma_4,\dots,\Sigma_{2n}$ in Σ_1. For $n = 3$ finding p^1_2 is identical to solving Problem 1(b) in reference frame Σ_1, using the procedure presented in Section IVC. We further can compute R^1_2 using any equation of the following form:

$$p^1_{2i} = p^1_2 + R^1_2 p^2_{2i}, \qquad i \in \{1,\dots,n\}. \tag{2}$$

It is obvious that the origins of the reference frames $\Sigma_1,\dots,\Sigma_{2n-1}$ form a complete graph, as do the origins of $\Sigma_2,\dots,\Sigma_{2n}$. For $n \geq 4$, these two complete graphs are connected with $n \geq 4$ edges (note that these edges do not share any vertex with each other.) From [30]

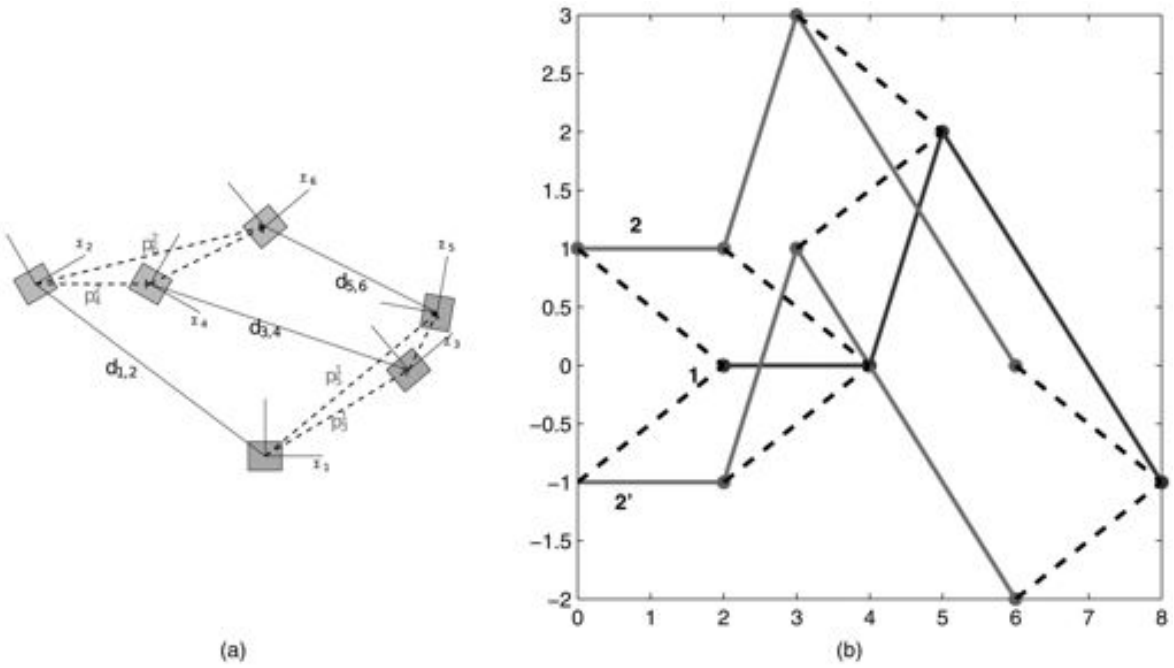

Fig. 3. (a) Setting considered in Problem 2. (b) Nongeneric case where 2 solutions exist for pose determination problem.

we know that the resulting graph is a globally rigid graph. Hence, the resulting formation when the origins of $\Sigma_1, \ldots, \Sigma_{2n-1}$ are considered anchors has a unique localization solution. As a result, due to the fact that there is a unique rotation relating Σ_1 to Σ_2, the agent-to-agent relative pose can be uniquely determined. We note that in [25] the authors have suggested a maximum of 4 solutions for Problem 2 when $n = 4$ and with probability one, only one of the solutions can be valid. Above we have shown, without appealing to probability, the following result:

COROLLARY 1 *For $n \geq 4$ Problem 2 has a unique solution (generically).*

One nongeneric scenario is when both agents move on a straight line [25]. Another nongeneric scenario is when the agents have the same displacement between any two consecutive measurements (see Fig. 3(b)). In these cases there are two distinct solutions for Problem 2.

VII. GEOMETRIC SENSITIVITY ANALYSIS

In the next several paragraphs, we argue that the singular values of a certain Jacobian matrix are relevant in describing bad geometries for localization.

First, we need to explain what is meant by a bad geometry. In the localization problem we have been considering, the measured information comprises three angles and three distances. From these, we seek to compute the positions of the agents. We have described how, in general, there are a finite number of solutions to this localization problem. We can envisage that supplementary data may enable a particular solution to be identified as the correct one, perhaps because the positions of all the agents were known a short while previously, and constraints on their speeds imply that only one solution in the finite set of possible solutions could be reached.

Now suppose that the measurements used to perform this localization are subject to noise. Then use of the localization algorithm will generate a set of agent positions that do not correspond to the correct values. One would hope that if the noise is small, the agent position errors will be small (the separate question of determining which positions from a finite set of possibilities having been dealt with through some form of supplementary information). However, for certain geometries, it may be that a small error in the measurements causes a large error in the localized position. Such geometries are what we term (qualitatively) bad geometries.

Denote the noiseless mapping from agent positions (a vector in $\mathbb{R}^{2n}$) to measurements (another vector in $\mathbb{R}^{2n}$) by F, where n is the number of agents. Let G be the inverse mapping. Let $\Delta(\cos\lambda)$ and Δd^2 denote errors in $\cos\lambda$ and d^2 due to the noise in measurements (d and λ) where d^2 and $\cos\lambda$ are vectors containing d_{ij}^2 and $\cos\lambda_i$, respectively. Let J_G denote the Jacobian of the mapping G. Let Δz denote the vector of adjustments to position estimates on account of the noise in the measurements. Then to first order there holds:

$$\begin{aligned}\Delta z &= J_G \begin{bmatrix} \Delta(\cos\lambda) \\ \Delta d^2 \end{bmatrix} \\ &= J_G \begin{bmatrix} -\Delta\lambda(\sin\lambda) \\ 2d\Delta d \end{bmatrix}. \end{aligned} \tag{3}$$

Assume that the errors in the λ_i are independent, of zero mean, and of variance σ_λ^2 while those in the d_{ij} are independent, zero mean, and of variance σ_d^2. Then it follows easily that

$$\begin{aligned}
&E[\Delta z^\top \Delta z] \\
&\quad = E\left\{ [\Delta(\cos\lambda)^\top \quad \Delta d^{2\top}] J_G^\top J_G \begin{bmatrix} \Delta(\cos\lambda) \\ \Delta d^2 \end{bmatrix} \right\} \\
&\quad = E\left\{ \mathrm{Tr}[J_G^\top J_G] \begin{bmatrix} \Delta(\cos\lambda) \\ \Delta d^2 \end{bmatrix} [\Delta(\cos\lambda)^\top \quad \Delta d^{2\top}] \right\} \\
&\quad = E\left\{ \mathrm{Tr}[J_G^\top J_G] \begin{bmatrix} -\Delta\lambda(\sin\lambda) \\ 2d\Delta d \end{bmatrix} \right. \\
&\qquad \left. \times [(-\Delta\lambda\sin\lambda)^\top \quad (2d\Delta d)^\top] \right\}. \qquad (4)
\end{aligned}$$

To first order, this is

$$E[\Delta z^\top \Delta z] = \mathrm{Tr}\{[J_G^\top J_G]\mathrm{diag}[\sin^2\lambda_i \sigma_\lambda^2, 4d_{ij}^2\sigma_d^2]\} \qquad (5)$$

Now what is a bad geometry? A sufficient condition to have a bad geometry occurs when the mean square estimated position error is large, even when the measurement errors are not large. If we make the assumption that all angles are bounded away from zero and π radians, that the values of d_{ij} remain in a bounded interval,and that there is non-zero measurement noise in angles and distances, it is evident that we need to avoid $\mathrm{Tr}[J_G^\top J_G]$ being large. Equivalently, the largest singular value of J_G should not be large, or equivalently again, the smallest singular value of J_F should not be small.

Sensitivity here is analogous to a geometric dilution of precision, and it is standard [31] not to use a condition number to measure that, but rather a singular value or trace.

Now we do the calculations where $n = 3$; however it is straightforward to extend the results obtained here to larger n. Let us start by introducing F and calculate J_F. Let d_{ij} denote the distance between T_i and T_j. Additionally, the position of T_i, $i = 1,2,3$ is denoted by $p_{T_i} = [x_{T_i}, y_{T_i}]^\top$. We assume that landmarks L_1 and L_2 are at positions $[0,1]^\top$ and $[0,-1]^\top$, respectively.

We have

$$\begin{aligned}
\cos\lambda_i &= \frac{x_{T_i}^2 + y_{T_i}^2 - 1}{(x_{T_i}^2 + (y_{T_i}+1)^2)^{1/2}(x_{T_i}^2 + (y_{T_i}-1)^2)^{1/2}} \\
&= g_i(p_1, p_2, p_3) \qquad (6) \\
D_{ij} &= d_{ij}^2 = (x_{T_i} - x_{T_j})^2 + (y_{T_i} - y_{T_j})^2 \\
&= f_{ij}(p_1, p_2, p_3).
\end{aligned}$$

Hence,

$$F(p_{T_1}, p_{T_2}, p_{T_3}) = \begin{bmatrix} g_1(p_{T_1}, p_{T_2}, p_{T_3}) \\ g_2(p_{T_1}, p_{T_2}, p_{T_3}) \\ g_3(p_{T_1}, p_{T_2}, p_{T_3}) \\ f_{12}(p_{T_1}, p_{T_2}, p_{T_3}) \\ f_{13}(p_{T_1}, p_{T_2}, p_{T_3}) \\ f_{23}(p_{T_1}, p_{T_2}, p_{T_3}) \end{bmatrix}. \qquad (7)$$

Furthermore,

$$\frac{\partial f_{ij}}{\partial x_{T_i}} = -\frac{\partial f_{ij}}{\partial x_{T_j}} = 2(x_{T_i} - x_{T_j}) \qquad (8)$$

$$\frac{\partial f_{ij}}{\partial y_{T_i}} = -\frac{\partial f_{ij}}{\partial y_{T_j}} = 2(y_{T_i} - y_{T_j}) \qquad (9)$$

$$\frac{\partial f_{ij}}{\partial x_{T_k}} = -\frac{\partial f_{ij}}{\partial y_{T_k}} = 0 \qquad (10)$$

$$\frac{\partial g_i}{\partial x_{T_j}} = \frac{\partial g_i}{\partial y_{T_j}} = \frac{\partial g_i}{\partial x_{T_k}} = \frac{\partial g_i}{\partial y_{T_k}} = 0 \qquad (11)$$

$$\frac{\partial g_i}{\partial x_{T_i}} = \frac{4x_{T_i}(x_{T_i}^2 - y_{T_i}^2 + 1)}{(x_{T_i}^2 + (y_{T_i}+1)^2)^{3/2}(x_{T_i}^2 + (y_{T_i}-1)^2)^{3/2}} \qquad (12)$$

$$\frac{\partial g_i}{\partial y_{T_i}} = \frac{8x_{T_i}^2 y_{T_i}}{(x_{T_i}^2 + (y_{T_i}+1)^2)^{3/2}(x_i^2 + (y_{T_i}-1)^2)^{3/2}} \qquad (13)$$

where $i, j, k \in \{1,2,3\}$. Hence, we have the following relationship between the perturbation in the measurements and the perturbation in the positions,

$$\begin{aligned}
&[\partial\lambda_1, \partial\lambda_2, \partial\lambda_3, \partial D_{12}, \partial D_{13}, \partial D_{23}]^\top \\
&\quad = J_F [\partial x_{T_1}, \partial y_{T_1}, \partial x_{T_2}, \partial y_{T_2}, \partial x_{T_3}, \partial y_{T_3}]^\top \qquad (14)
\end{aligned}$$

where J_F is,

$$J_F = \begin{bmatrix}
-\csc\lambda_1 \dfrac{\partial g_1}{\partial x_{T_1}} & -\csc\lambda_1 \dfrac{\partial g_1}{\partial y_{T_1}} & 0 & 0 & 0 & 0 \\
0 & 0 & -\csc\lambda_2 \dfrac{\partial g_2}{\partial x_{T_2}} & -\csc\lambda_2 \dfrac{\partial g_2}{\partial y_{T_2}} & 0 & 0 \\
0 & 0 & 0 & 0 & -\csc\lambda_3 \dfrac{\partial g_3}{\partial x_{T_3}} & -\csc\lambda_3 \dfrac{\partial g_3}{\partial y_{T_3}} \\
2(x_{T_1} - x_{T_2}) & 2(y_{T_1} - y_{T_2}) & 2(x_{T_2} - x_{T_1}) & 2(y_{T_2} - y_{T_1}) & 0 & 0 \\
2(x_{T_1} - x_{T_3}) & 2(y_{T_1} - y_{T_3}) & 0 & 0 & 2(x_{T_3} - x_{T_1}) & 2(y_{T_3} - y_{T_1}) \\
0 & 0 & 2(x_{T_2} - x_{T_3}) & 2(y_{T_2} - y_{T_3}) & 2(x_{T_3} - x_{T_2}) & 2(y_{T_3} - y_{T_2})
\end{bmatrix}. \qquad (15)$$

THEOREM 7 *The Jacobian J_F given in* (15) *is well defined if $x_{T_i} \neq 0$, $\forall i = 1,2,3$, and is singular given that $x_{T_i} \neq 0$, $\forall i = 1,2,3$, if*

$$\det\left(\begin{bmatrix} x_{T_1} - \cot\lambda_1 & x_{T_2} - \cot\lambda_2 & x_{T_3} - \cot\lambda_3 \\ y_{T_1} & y_{T_2} & y_{T_3} \\ \cot\lambda_1 y_{T_1} & \cot\lambda_2 y_{T_2} & \cot\lambda_3 y_{T_3} \end{bmatrix}\right) = 0. \tag{16}$$

PROOF See Appendix II.

Theorem 7 states that in 6-dimensional space defined by x_{T_i} and y_{T_i}, $i = 1,2,3$, there exists a hypersurface defined by (16) where the Jacobian matrix J_F is singular. It is easy to see that when the angles are equal this determinant is zero, hence J_F is singular. However, this condition is not necessary for the determinant to be zero. So there exist bad geometries other than the case where the angles are equal. When two landmarks are replaced by three or more, another approach becomes possible; see the next section. Note however that it is still feasible to work with the Jacobian, which is now a tall matrix, and again bad geometries correspond to there being a singular value close to 0. Additional measurements lower the likelihood of this occurring.

VIII. AGENT LOCALIZATION IN THE PRESENCE OF NOISE

In this section we propose a method for localizing the agents in the presence of noise for the cases that a unique localization solution exists. In the next subsection we address the problem of localization of a formation of three UAVs measuring the subtended angle at them by three landmarks in the presence of noise. Later in this section we address the problem of pose determination using noisy distance measurements.

A. Localization in the Presence of Noise and Extra Landmarks

When there are three agents and two landmarks, there is no special technique for dealing with the noise. One simply proceeds using noisy measurements in lieu of noiseless measurements. However, when the noiseless equations are overdetermined, as for example with three landmarks, a modified method is required to handle the equations.

First we consider the scenario described in Section VA, temporarily assuming there is no measurement noise. As described before for each agent and any selection of two landmarks, we can define a circle. Call the center and the radius of the circle defined by T_i, L_1 and L_2, $A_i = [x_i, y_i]^\top$ and R_i, respectively; term the center and the radius of the circle defined by T_i, L_1 and L_3, $A'_i = [x'_i, y'_i]^\top$ and R'_i, and term the center and the radius of the circle defined by T_i, L_2 and L_3, $A''_i = [x''_i, y''_i]^\top$ and R''_i. All the equations that govern the system can be written as

$$\begin{aligned}
&(x_{T_i} - x_i)^2 + (y_{T_i} - y_i)^2 - R_i^2 = 0, && i \in \{1,2,3\} \\
&(x_{T_i} - x'_i)^2 + (y_{T_i} - y'_i)^2 - R_i'^2 = 0, && i \in \{1,2,3\} \\
&(x_{T_i} - x''_i)^2 + (y_{T_i} - y''_i)^2 - R_i''^2 = 0, && i \in \{1,2,3\} \\
&(x_{T_i} - x_{T_j})^2 + (y_{T_i} - y_{T_j})^2 - r_{ij}^2 = 0, && i,j \in \{1,2,3\}
\end{aligned} \tag{17}$$

where $p_{T_i} = [x_{T_i}, y_{T_i}]^\top$ is the position of agent T_i. It is obvious that (17) has a unique set of solutions for the positions of the T_i. This solution is a root of the following polynomial.

$$\begin{aligned}
P = &\sum_{i=1}^{3}((x_{T_i} - x_i)^2 + (y_{T_i} - y_i)^2 - R_i^2)^2 \\
&+ \sum_{i=1}^{3}((x_{T_i} - x'_i)^2 + (y_{T_i} - y'_i)^2 - R_i'^2)^2 \\
&+ \sum_{i=1}^{3}((x_{T_i} - x''_i)^2 + (y_{T_i} - y''_i)^2 - R_i''^2)^2 \\
&+ \sum_{i,j\in\{1,2,3\}}((x_{T_i} - x_{T_j})^2 + (y_{T_i} - y_{T_j})^2 - r_{ij}^2)^2.
\end{aligned} \tag{18}$$

Furthermore, it is easy to show that this solution is the global minimizer of (18) as well. Hence, the solution, $p_T^* = [p_{T_1}^{*\top}, p_{T_2}^{*\top}, p_{T_3}^{*\top}]^\top$ is obtained by

$$p_T^* = \arg\min P. \tag{19}$$

Now assume that the measurement is noisy, hence (17) does not necessarily have a solution, however in the light of introduction of (18) one can solve the minimization equation to obtain an estimate for the solution. We describe how to solve this minimization problem in Appendix III. In what follows we show the corresponding reformulation of the problem introduced in Section VI.

B. Noisy Relative Reference Frame Determination

We already mentioned that Problem 2 has a unique solution, where there are 4 or more measurements. Here we consider the case where we have $n \geq 4$ measurements. The following set of equations govern the system for calculating p_2^1 and R_2^1 when we have range measurements $d_{2i-1,2i}$ available.

$$\|p_{2i-1}^1 - p_{2i}^1\|^2 = d_{2i-1,2i}^2, \qquad i \in \{1,\ldots,n\}. \tag{20}$$

Replacing p_{2i}^1 with the right-hand side of (2) we have

$$\|p_{2i-1}^1 - R_2^1 p_{2i}^2 - p_2^1\|^2 = d_{2i-1,2i}^2, \qquad i \in \{1,\ldots,n\} \tag{21}$$

where

$$R_2^1 = \begin{bmatrix} \cos\phi & \sin\phi \\ -\sin\phi & \cos\phi \end{bmatrix}.$$

Moreover, substituting $\sin\phi$ and $\cos\phi$ with x_s and x_c transforms it into a system of polynomial equations

$$\begin{aligned} \|p^1_{2i-1} - R^1_2 p^2_{2i} - p^1_2\|^2 &= d^2_{2i-1,2i}, \qquad i \in \{1,\dots,n\} \\ x_s^2 + x_c^2 &= 1. \end{aligned} \tag{22}$$

The solution to (22) where p^1_2, x_c, and x_s are unknown, and $d_{2i-1,2}$ and p^2_{2i} are known, $p^* = [p^{1*\top}_2, x^*_s, x^*_c]$is a root of the following system of polynomials as well,

$$P' = \sum_{i=1}^{n} (\|p^1_{2i-1} - R^1_2 p^2_{2i} - p^1_2\|^2 - d^2_{2i-1,2i})^2 \tag{23}$$

$$x_s^2 + x_c^2 = 1. \tag{24}$$

And similarly to before, it is easy to show that this solution is the global minimizer of (23) as well So the solution p^* is obtained by

$$\begin{aligned} p^* &= \arg\min_{p^1_2, x_c, x_s} P' \\ &\text{subject to} \quad x_s^2 + x_c^2 = 1 \end{aligned} \tag{25}$$

where $\sin\phi^* = x^*_s$ and $\cos\phi^* = x^*_c$.Again in the presence of noise (20) does not have a solution, and the best estimate can be obtained by solving (25).

REMARK 4 Note that the constraint $x^{*2}_s + x^{*2}_c = 1$ is required to obtain a plausible rotation matrix and cannot be considered as part of the cost function. It should be satisfied explicitly.

We minimize the polynomial cost functions introduced here and find their global minimizers using sum of squares (SOS) relaxation. We briefly describe the method that we use in Appendix III, and point out the important references regarding this method.

REMARK 5 Note that adding more measurements would not change the number of the unknown variables and the degree of the cost function P'. Hence the complexity of solving the optimization problem (25) would not change by adding new measurements.

IX. SIMULATIONS AND EXPERIMENTS

In this section a set of simulation and real robot experimentation results are presented to show different localization solutions in different scenarios. In the real robot experimentation studies, e-puck robots [32] and an overhead camera are used in a 320 cm by 250 cm indoor environment. The first subsection below considers the problem of localizing a formation of 3 UAVs that can measure the subtended angle by two landmarks on them. The second subsection considers the problem of robot-to-robot frame localization in the presence of noise. However, before proceeding to the results we first introduce the odometry model for the robot that we use here, i.e., e-puck. E-puck is a differential drive robot and the position of such a robot at time step k, $p(k) = [x_p(k), y_p(k), \theta_p(k)]^\top$, where $x_p(k)$, $y_p(k)$, and $\theta_p(k)$ are the x-coordinate, the y-coordinate, and the heading of the robot, respectively, can be estimated by looking at the difference in the encoder values of the left and the right wheel, Δs_l and Δs_r, respectively. The sampling rate of the robot is 7KHz [32], and after each time step the position is

$$p(k+1) = p(k) + \Delta p$$

where $\Delta p = [\Delta x_p, \Delta y_p, \Delta\theta_p]^\top$, and

$$\Delta\theta_p = \frac{\Delta s_l - \Delta s_r}{b}$$

$$\Delta x_p = \Delta s \cos\left(\theta_p(k) + \frac{\Delta\theta_p}{2}\right)$$

$$\Delta y_p = \Delta s \sin\left(\theta_p(k) + \frac{\Delta\theta_p}{2}\right)$$

$$\Delta s = \frac{\Delta s_l + \Delta s_r}{2}$$

and b is the distance between the wheels. For information on introducing noise in the above model see [33].

A. Three UAV Formation Localization

In this section we present some simulation results for validating our methods for solving the first problem discussed in the paper. First we consider the case where there are 3 agents and 2 landmarks and study different scenarios (involving some with noise). Later we consider the case where an extra landmark is available and the measurements are noisy.

1) *Simulations with 3 Agents and 2 Landmarks*: The angle and distance values used in each simulation scenario are presented in Table I. In addition, it is worth mentioning that after running numerous simulations, a case with twelve localization solutions was never encountered.

The important characteristics of each simulation result and the number of localization solution in each scenario are presented in Table II. The legends used in simulation results are described in Table III. In Fig. 4(a) and Fig. 4(b) two scenarios where respectively 4 and 8 localization solutions exist are presented. A nongeneric case is presented in Fig. 5(a), where there are repeated localization solutions. A bad geometry is identified in Fig. 5(b), where an infinite number of localization solutions exists. This infinite localization ambiguity occurs if the three agents and the two landmarks lie on a common circle. Please note

TABLE I
The Angle and Distance Values in Each Scenario

Scenario	λ_1 (rad)	λ_2 (rad)	λ_3 (rad)	$\overline{T_1T_2}$ (m)	$\overline{T_1T_3}$ (m)	$\overline{T_2T_3}$ (m)
Fig. 4(a)	1.0472	0.6283	0.5236	1	1	1
Fig. 4(b)	0.3805	0.2526	0.1674	3.1623	5.099	2.8284
Fig. 5(a)	1.0472	0.8976	0.7854	1.5	0.9765	1.25
Fig. 5(b)	0.2487	0.2487	0.2487	2.0859	2.7552	4.6188

TABLE II
The Number of Localization Solutions in Each Scenario and Important Characteristics of Each Scenario

Scenario	No. of Distinct Solutions	Characteristic
1 (Fig. 4(a))	4	generic
2 (Fig. 4(b))	8	generic
3 (Fig. 5(a))	2	nongeneric/repeated solutions
4 (Fig. 5(b))	infinite	nongeneric/infinite ambiguity

TABLE III
The Legends used in Simulation Results

agent	small solid circle
landmark	solid diamond
formation	solid triangles
agent locus	dashed circles
coupler curve	dotted curves

that for all the scenarios the landmarks L_1 and L_2 are placed at $[0,1]^\top$ and $[0,-1]^\top$, respectively.

2) *Experiment with 3 Mobile Robots and 2 Landmarks*: In this section we study the application of Algorithm 1 for localizing a formation of 3 mobile agents capable of measuring the angles subtended at each of these agents by two landmarks. We used 3 e-puck robots in a 320 cm by 250 cm environment. The measurements are carried out using an overhead camera. The actual angle measurements are corrupted by a zero mean Gaussian error with a variance equal to 0.01 rad^2, and inter-agent distance measurements noise is considered to be zero mean Gaussian with variance equal to 1 cm^2. The landmarks are placed at $[0,20]^\top$ and $[0,220]^\top$. In 9 different instants of time while at each of these instants there are generically multiple solutions here the average of the closest localization solution to the real solution over 20 repetitions of the same experiment is depicted as stars in Fig. 6 (in each repetition the synthetic measurements are corrupted by a different noise value.). Furthermore, the paths that the robots move on are presented as solid lines in Fig. 6. Moreover, the mean values of the closest estimated position and the corresponding variances are presented in Table V. In addition the average of the absolute error between estimate and true values for all time instants during this experiment for agents T_1, T_2, and T_3 are respectively 16.2152, 8.7560, and 8.5412. This value for each time instant is presented in Table IV. Comparing the values in these two tables will lead us to concluding that there is a large bias in the estimates in this scenario.

3) *Simulations with Multiple Agents and 2 Landmarks*: In this simulation we consider 3 different scenarios, where the formation is comprised of 4, 5, and 6 agents and can measure the subtended angle at them by two landmarks. In each scenario we consider 5 different noise levels in the measurements of subtended angle at each of the agents by any two landmarks and we have run the simulation with each noise level for 20 times. At the end of each 20 times run of the simulation with a noise level we have averaged the norm of the absolute error between the real position of the agents and their estimates. These average values obtained from different noise levels and the different number of landmarks is depicted in Fig. 7.

4) *Simulations with 3 Agents and Multiple Landmarks*: Here we consider that the exact position of agents 1, 2 ,and 3 are respectively $[5,-3]^\top$, $[2,1]^\top$, and $[1,4]^\top$ (the positions are in meters). We consider 3 different scenarios, where 3, 4, and 5 landmarks are available. In each scenario we consider 5 different noise levels in the measurements of subtended angle at each of the agents by the landmarks and we have run the simulation with each noise level for 20 times. At the end of each 20 times run of the simulation with a noise level we have averaged the norm of the absolute error between the real position of the agents and their estimates. These average values obtained from different noise levels and the different number of landmarks is depicted in Fig. 8.

5) *Variation of Sensitivity to Noise with Respect to Changing the Position of One Agent*: In this scenario we study the effect of different formation settings on the minimum singular value of the Jacobian matrix J as described by (15). We assume that the landmarks are at $[0,10]^\top$ and $[0,-10]^\top$, and two of the agents are at fixed positions $[20,30]^\top$ and $[40,-30]^\top$. We assume that the third agent moves on the horizontal line $y = 0$ and is moving away from the landmarks. The minimum singular value of the Jacobian matrix changes as the agents move; this variation is presented in Fig. 9(a). As it is clear from the figure, when $x_{T_3} = 60$, the singular value goes to zero, suggesting a high sensitivity to noise value.

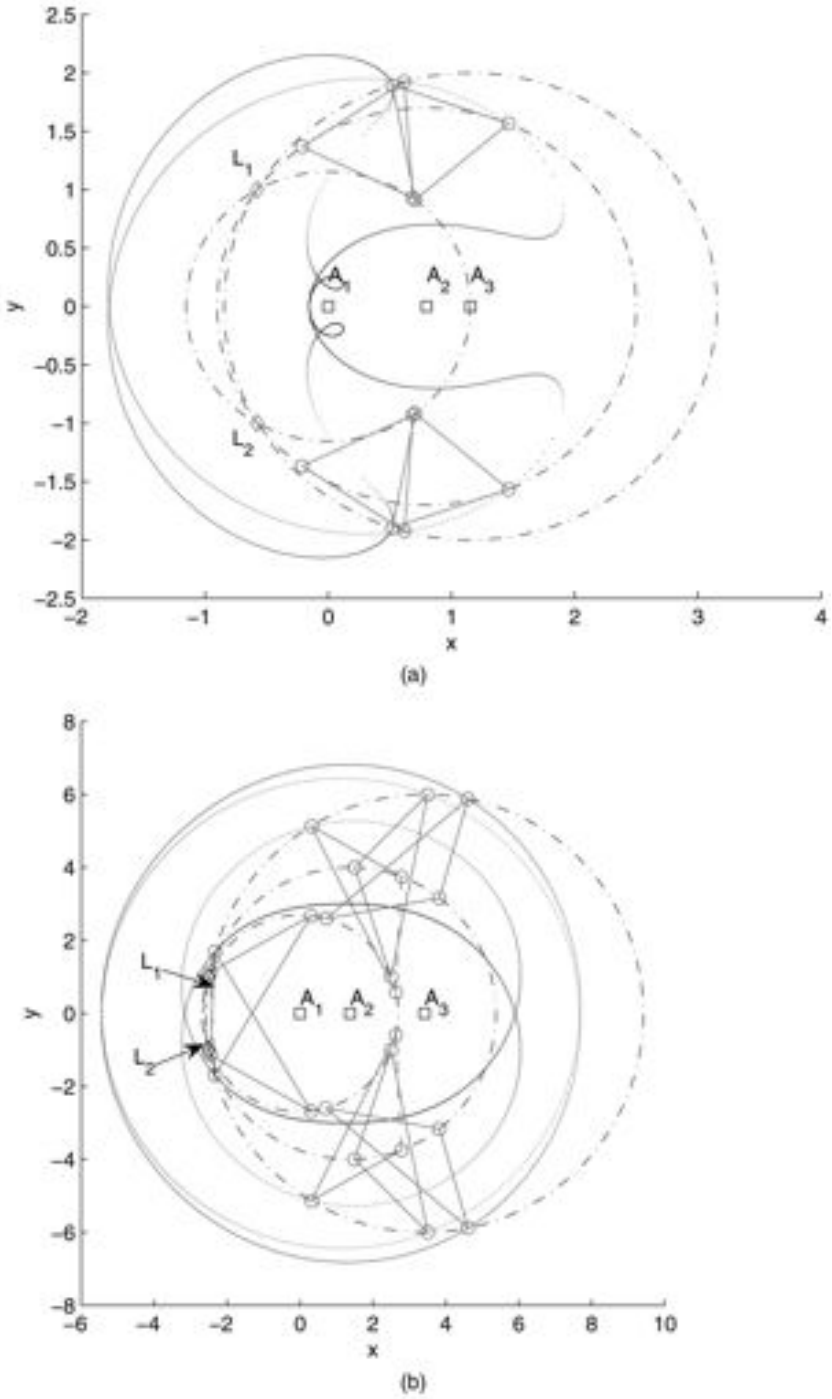

Fig. 4. (a) Possible localization solutions for scenario 1 as described in Table II. (b) Possible localization solutions for scenario 2 as described in Table II.

After calculating λ_i, $i = 1,2,3$ at this point it becomes obvious that all the angles are equal to 0.32 rad which constitutes a bad geometry as described earlier. Later, we change both of the coordinates of T_3 in a $[0,100] \times [-50,50]$ square region. The variation of the minimum singular value of the Jacobian matrix is presented in Fig. 9(b). This figure shows in which T_3 the localization solution is less sensitive to the noisy measurements, i.e., where the minimum singular value is larger.

B. Robot-to-Robot Reference Frame Determination in the Presence of Noise

In this section we consider the case of robot-to-robot reference frame determination where the measurements are noisy. First we show the result in a simulation then we show the application of the method in an experimental setting.

1) *Simulations*: In the first scenario that we consider, $p_3^1 = [2.0407, -0.9862]^\top$, $p_5^1 = [3.0233, 1.9054]^\top$, $p_7^1 = [4.0186, 0.9239]^\top$, $d_{12} =$

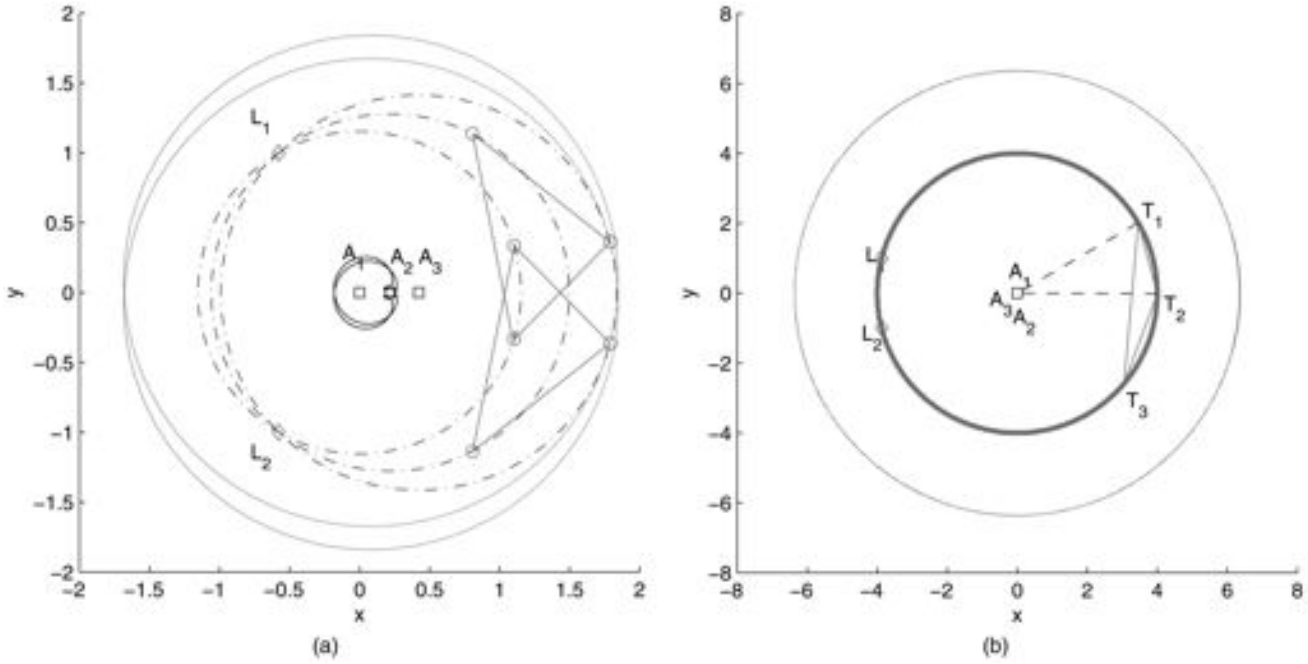

Fig. 5. (a) Repeated localization solutions. (Scenario 3 as described in Table II.) (b) Infinite number of localization solutions for scenario 4 as described in Table II. Locus of T_3 coincides with one of the branches of the coupler curve.

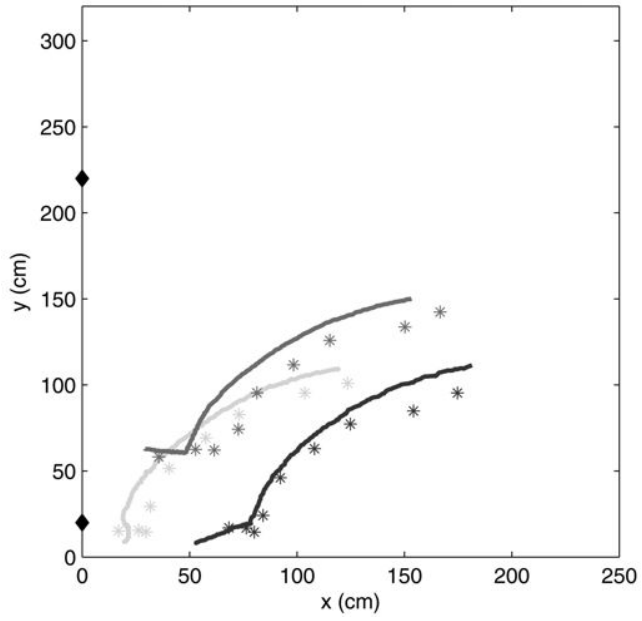

Fig. 6. Robots trajectories and nearest estimate obtained by Algorithm 1.

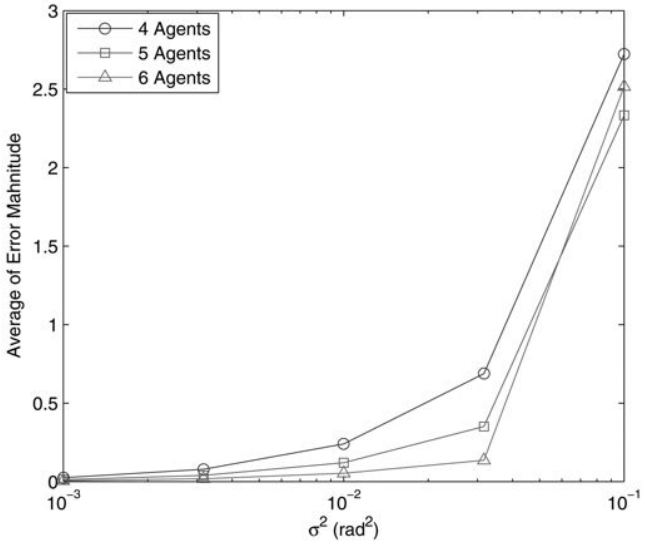

Fig. 7. The effect of different number of agents and different noise levels on average of absolute error between exact position of agents and their estimates.

7.1626, $d_{34} = 5.9512$, $d_{56} = 6.6932$, $d_{78} = 5.0052$, $p_4^2 = [1.0555, -1.9487]^\top$, $p_6^2 = [5.0235, 0.9997]^\top$, and $p_8^2 = [7.0963, -3.1266]^\top$. The distance measurements are noisy, and the noise is considered to be a random Gaussian variable with zero mean and variance equal to 0.1 m^2. Solving the optimization problem corresponding to this pose determination problem we obtain, $p_2^{1*} = [1.2479, 7.0525]^\top$, and $\phi = 0.0312$ rad. Comparing with the real values $p_2^1 = [1, 7]^\top$ and $\phi = 0$, we observe that estimates are very close to the real values.

In the second scenario we aim to study the effect of different levels of noise in distance measurements and odometry readings on the solution. First we set the distance measurement variance equal to 0.1 m^2 and set the noise variance on odometry readings 0.0001 m^2. After repeating the procedure 100 times, the average of the absolute error bewteen estimate and true values $\|p_2^{1*} - p_2^1\|$ is 0.2665 m, and the average of the angle estimate error, $|\phi^* - \phi|$ is 0.0311 rad. Then we set the distance measurement variance equal to 0.0001 m^2 and set the noise on odometry readings 0.1 m^2. After repeating the procedure 100 times, the

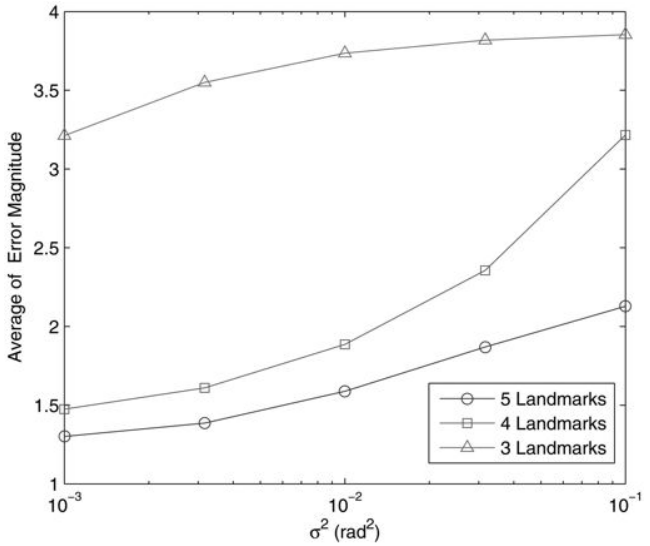

Fig. 8. Effect of different number of landmarks and different noise levels on average of absolute error between exact position of agents and their estimates.

average of the absolute error bewteen estimate and true values, $\|p_2^{1*} - p_2^1\|$, is 0.4078 m, and the average of the angle estimates error $|\phi^* - \phi|$ is 0.0385 rad. While the average errors of the angle estimate in the two cases are close, the average of the absolute error bewteen estimate and true values is somewhat larger in the second scenario with larger odometry error, suggesting it to be more problematic.

2) *Experiment with 2 Mobile Robots*: In this section we apply the method introduced in Section VIIIB to an experimental setting. We used 2 e-puck robots in a 320 cm by 250 cm environment. To measure distances between the robots an overhead camera is used and the distance measurement

TABLE IV
The Average of the Absolute Error Bewteen Estimate and True Values for 9 Time Instants after Repetition of the Experiment for 20 Times, via Corrupting the Synthetic Measurements by 20 Different Noise Values

Time Instant	Error Magnitude Mean for T_1	Error Magnitude Mean for T_2	Error Magnitude Mean for T_3
1	7.2399	4.8804	1.4737
2	6.5246	5.1696	2.1418
3	14.7415	9.7683	5.1983
4	19.0578	10.3529	10.1608
5	15.7964	6.8016	7.9873
6	16.8809	7.9409	8.8000
7	14.7863	6.3368	10.8410
8	29.0844	15.1950	16.2922
9	21.8252	12.3584	13.9760

obtained from the camera is further corrupted by a zero mean Gaussian error with a variance equal to 4 cm^2. The displacement of the robots between each two consecutive stops is measured by adding encoder readings in short intervals of time. The robots trajectories are depicted in Fig. 10. The values of p_2^{1*} and ϕ^* using 4 and 5 measurements are presented in Table VI. Furthermore, the differences between these values and the values obtained from the overhead camera are presented for comparison.

3) *Comparison of the Result with that of [25]*: In both cases the problems are defined considering the same hypotheses. The first difference is in the solution count where 4 measurements are available. Here using the result from graph rigidity we have proven that the number of solutions must be one for generic positions of the robots where 4 or more measurements are available. The second difference

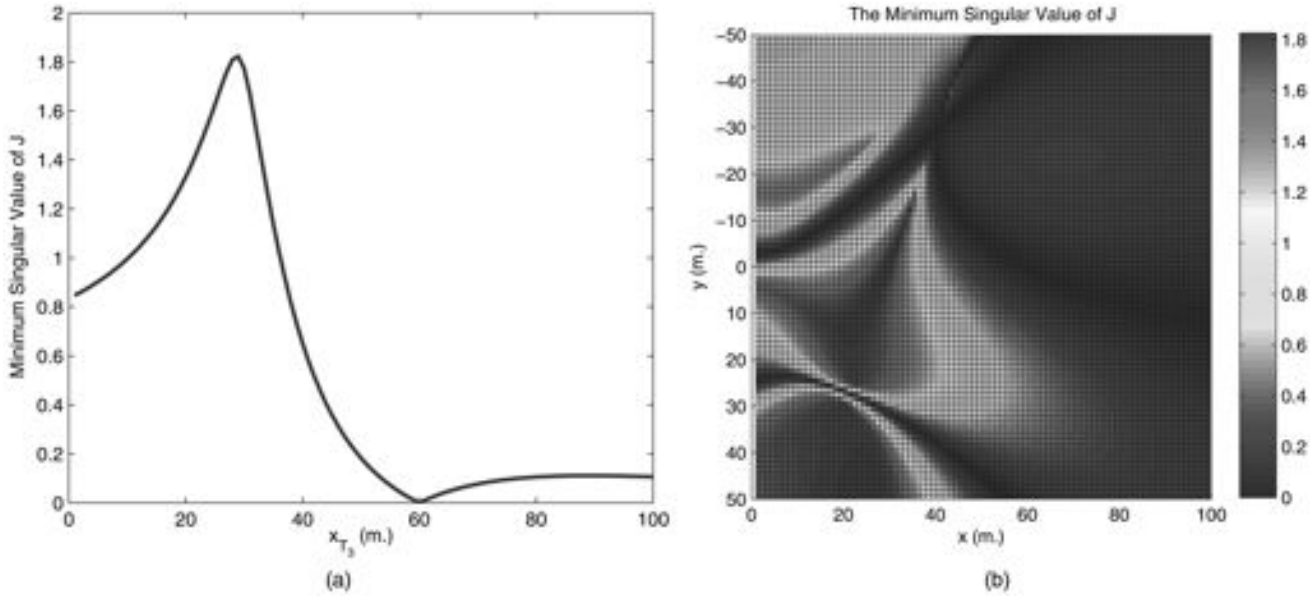

Fig. 9. Variation of minimum singular of value of J with respect to changes in position of T_3. (a) T_3 moving on horizontal line. (b) T_3 in 100 by 100 square region.

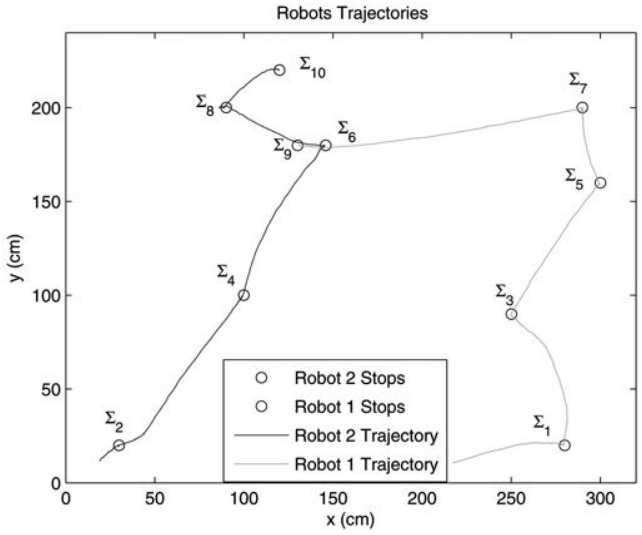

Fig. 10. Robots trajectories in experiment of Section IXB2.

originates from the approaches to tackle the problem. In [25] a linear method is used to calculate the solution to the problem while here a nonlinear method (taking the geometry and neighborhood topology into account explicitly) has been used. Furthermore in the localization literature the potential high sensitivity of linear algorithms to small amounts of noise has been recorded, e.g. see [34], [35]. We have further compared the methods by feeding the same set of data to each of the algorithms (based on our understanding of the method introduced in [25]) for 100 rounds for 10 different levels of noise. The result is depicted in Fig. 11, where the method introduced here always

TABLE VI
Results from the Experiment of Section IXB2

No. Meas.	$p_2^{1^*}$ (cm)	ϕ^* (rad)	$\|p_2^{1^*} - p_2^1\|$ (cm)	$\|\phi^* - \phi\|$ (rad)
4	$\begin{bmatrix} -213.3462 \\ -128.4479 \end{bmatrix}$	0.0885	16.1709	0.0129
5	$\begin{bmatrix} -208.4538 \\ -136.2917 \end{bmatrix}$	0.0834	6.9265	0.0078

results in a lower error for estimating p_2^1 and ϕ for different noise levels. However, it is worth noting that the average time for running the method introduced in this paper is 17.17 s while the method in [25] takes 0.01 s in average, and hence the latter is very suitable for fast computations.

X. CONCLUDING REMARKS

In this paper an upper bound of 12 is obtained for the number of possible localization solutions of a triangular (3-agent) formation, collecting bearing measurements to two landmarks. Furthermore, a more general theorem regarding localization of globally rigid formations, taking advantage of a priori knowledge about the position of two landmarks, is presented. In addition, geometries that are highly sensitive to the noise are identified, e.g. when all angles subtended at each of the three agents by the two landmarks are equal, or equivalently, the three agents and the two landmarks are placed on the same circle. In this case there are an infinite number of

TABLE V
The Mean and Variance of the Closest Estimated Positions of the Agents T_i ($i = 1,2,3$) to Their Real Position for 9 Time Instants After Repetition of the Experiment for 20 Times, via Corrupting the Synthetic Measurements by 20 Different Noise Values

Time Instant	$[\bar{x}_{T_1}\ \bar{y}_{T_1}]^\top$	$[\bar{x}_{T_2}\ \bar{y}_{T_2}]^\top$	$[\bar{x}_{T_3}\ \bar{y}_{T_3}]^\top$
1	$[35.7048, 58.2244]^\top$	$[16.9291, 15.1095]^\top$	$[68.2769, 16.9451]^\top$
2	$[52.8116, 62.5552]^\top$	$[26.2991, 15.4873]^\top$	$[76.3441, 16.8744]^\top$
3	$[62.5250, 62.1531]^\top$	$[29.8062, 14.6213]^\top$	$[80.0897, 14.4910]^\top$
4	$[72.7187, 74.3254]^\top$	$[31.7637, 29.3865]^\top$	$[84.1796, 24.0888]^\top$
5	$[81.3115, 95.4220]^\top$	$[40.4582, 51.5817]^\top$	$[92.2197, 46.0260]^\top$
6	$[98.3628, 111.7192]^\top$	$[57.5488, 69.2409]^\top$	$[108.1229, 62.9297]^\top$
7	$[115.1997, 125.9023]^\top$	$[73.0674, 82.8402]^\top$	$[124.8187, 77.2636]^\top$
8	$[150.1768, 133.640]^\top$	$[103.6088, 95.3639]^\top$	$[154.2225, 84.9073]^\top$
9	$[166.5329, 142.4228]^\top$	$[123.5453, 100.9549]^\top$	$[174.6442, 95.3917]^\top$
Time Instant	**var(T_1)**	**var(T_2)**	**var(T_3)**
1	$[0.0784, 0.0043]^\top$	$[0.0052, 0.0017]^\top$	$[0.0047, 0.0013]^\top$
2	$[0.1815, 0.0651]^\top$	$[0.0687, 0.0241]^\top$	$[0.0690, 0.1871]^\top$
3	$[0.1792, 0.1008]^\top$	$[0.0411, 0.0270]^\top$	$[0.0406, 0.2201]^\top$
4	$[0.6046, 0.1107]^\top$	$[0.2158, 0.0044]^\top$	$[0.1858, 0.1772]^\top$
5	$[3.5479, 0.3010]^\top$	$[0.9768, 0.1844]^\top$	$[0.7673, 0.5900]^\top$
6	$[4.1536, 0.5165]^\top$	$[1.6546, 0.0580]^\top$	$[1.4166, 0.8567]^\top$
7	$[8.5006, 0.4361]^\top$	$[4.7366, 0.4418]^\top$	$[4.3804, 0.6814]^\top$
8	$[41.4915, 6.3180]^\top$	$[25.2545, .15865]^\top$	$[22.0723, 7.2126]^\top$
9	$[119.5962, 19.1815]^\top$	$[57.7045, 2.3364]^\top$	$[50.3592, 25.0818]^\top$

Note: $[\bar{x}_{T_i}\ \bar{y}_{T_i}]^\top$ is the mean of the estimated position for agent T_i, and var(T_i) denotes the variance of the estimated positions after running the experiment for 20 times.

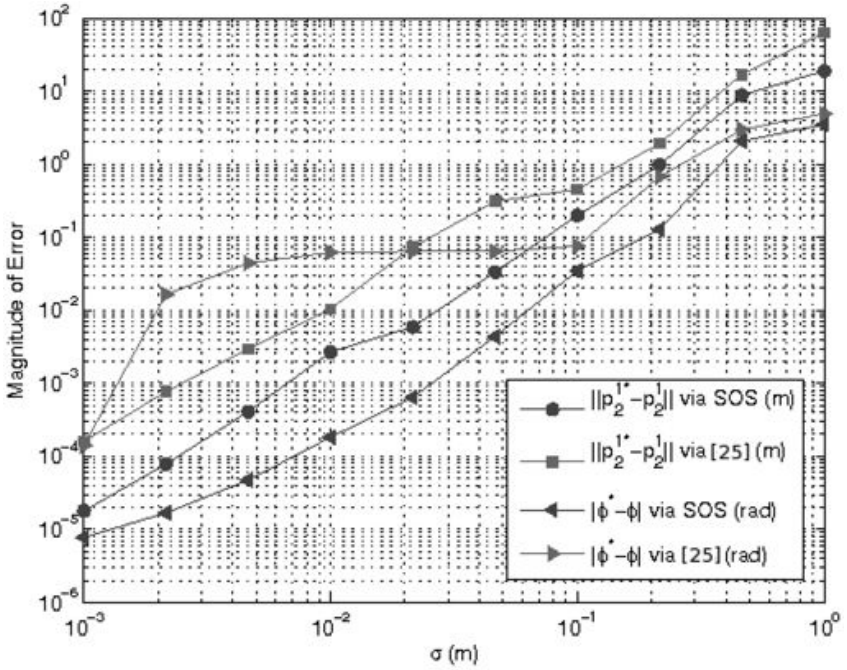

Fig. 11. Average of absolute error bewteen estimate and true values of p_2^1 and ϕ obtained from applying the methods introduced here and in [25] after 100 rounds.

localization solutions. Additionally, the effect of having extra landmarks and/or agents capable of measuring angles is studied in this paper. Moreover, the application of the theory developed in this paper to the problem of robot-to-robot relative reference frame determination in two-dimensional space using distance measurements is discussed. In the end some simulation and experimental results are presented.

APPENDIX I. PROOF OF THEOREM 6

Let the actual positions of T_1, T_2, T_3, and T_4 be $p_{T_1}^*$, $p_{T_2}^*$, $p_{T_3}^*$, and $p_{T_4}^*$, respectively. Given L_1, L_2, $\overline{T_1T_2}$, $\overline{T_1T_3}$, $\overline{T_2T_3}$, λ_1, λ_2, and λ_3 (or equivalently the centers A_1, A_2, and A_3 of the circumcircles of triangles $\triangle L_1T_1L_2$, $\triangle L_1T_2L_2$, and $\triangle L_1T_3L_2$), Theorem 4 implies that there exist at most 2×6 solutions for $T_1T_2T_3$, two of which are $p_{T_1}^*p_{T_2}^*p_{T_3}^*$ and $p_{T_1}^{*m}p_{T_2}^{*m}p_{T_3}^{*m}$, where $p_{T_i}^{*m}$ denotes the mirror image of $p_{T_i}^*$ ($i=1,2,3,4$) with respect to the line A_1A_2. Without loss of generality let solution 1 be $p_{T_1}^1p_{T_2}^1p_{T_3}^1 = p_{T_1}^*p_{T_2}^*p_{T_3}^*$, and solution 2, $p_{T_1}^2p_{T_2}^2p_{T_3}^2$, be a solution other than $p_{T_1}^*p_{T_2}^*p_{T_3}^*$ and $p_{T_1}^{*m}p_{T_2}^{*m}p_{T_3}^{*m}$, whose existence is guaranteed by Theorem 4.

Let us take T_4 into consideration as well: we are given $\overline{T_1T_4}$, $\overline{T_2T_4}$, and $\overline{T_3T_4}$, and λ_4 (or equivalently A_4 the center of circumcircle of $\triangle L_1T_4L_2$). Note that since $T_1T_2T_3T_4$ is globally rigid, for each i, there is a unique $p_{T_4}^i$ having distances $\overline{T_1T_4}$, $\overline{T_2T_4}$, and $\overline{T_3T_4}$ from, respectively, $p_{T_1}^i$, $p_{T_2}^i$, and $p_{T_3}^i$. Hence, $p_{T_4}^1 = p_{T_4}^*$ lies on the circle $C(A_4,\overline{A_4L_1})$, i.e., $\overline{A_4L_1} = \overline{A_4p_{T_4}^1}$.

Let Ψ_1^2 be the unique roto-translation mapping $\triangle p_{T_1}^1p_{T_2}^1p_{T_3}^1$ to $\triangle p_{T_1}^2p_{T_2}^2p_{T_3}^2$, and Ψ_2^1 be its unique inverse mapping that maps $\triangle p_{T_1}^2p_{T_2}^2p_{T_3}^2$ to $\triangle p_{T_1}^1p_{T_2}^1p_{T_3}^1$. Let $L_1^2 \triangleq \Psi_1^2(L_1)$, $L_2^2 \triangleq \Psi_1^2(L_2)$, and $A_i^2 \triangleq \Psi_1^2(A_i)$ for $i\in\{1,2,3,4\}$. Since Ψ_1^2 is roto-translation, A_1,A_2,A_3,A_4 are collinear, and $p_{T_4}^1$ lies on the circle $C(A_4,\overline{A_4L_1})$, we have the following:

1) A_1^2,A_2^2,A_3^2,A_4^2 are collinear,
2) $\overline{A_4^2L_1^2} = \overline{A_4L_1}$,
3) $\Psi_1^2(p_{T_4}^1) = p_{T_4}^2$ lies on the circle $C(A_4^2,\overline{A_4^2L_1^2})$.

To obtain a contradiction, assume that $p_{T_4}^2$ also lies on the circumcircle $C(A_4,\overline{A_4L_1})$ of $\triangle L_1T_4L_2$. Then, by 3) above, $p_{T_4}^2$ needs to be one of the at most two intersection points of the circles $C(A_4,\overline{A_4L_1})$ and $C(A_4^2,\overline{A_4^2L_1^2})$. For generic angles and distances, since these two circles are defined independently of $p_{T_4}^1$ and $p_{T_4}^2$, i.e., since $p_{T_4}^2$ can be any arbitrary point on $C(A_4^2,\overline{A_4^2L_1^2})$ (corresponding to $p_{T_4}^1 = \Psi_2^1(p_{T_4}^2)$ being a generic point on $C(A_4,\overline{A_4L_1})$), this last condition cannot be satisfied generically, which is a contradiction (see Fig. 12). Hence the only solutions for positions of $T_1T_2T_3T_4$ are $p_{T_1}^*p_{T_2}^*p_{T_3}^*p_{T_4}^*$ and $p_{T_1}^{*m}p_{T_2}^{*m}p_{T_3}^{*m}p_{T_4}^{*m}$.

APPENDIX II. PROOF OF THEOREM 7

For the case where $\exists i=1,2,3$ such that $x_{T_i}=0$, $\cot\lambda_i$ is not defined and hence the Jacobian matrix J_F is not well defined. Assuming for $x_{T_i}\neq 0$, $\forall i=1,2,3$, from (6) and since it is assumed that we know which side of the landmarks the agents are assume $x_{T_i}\geq 0$

and $\lambda_i \in (0,\pi]$, we obtain

$$\sin\lambda_i = \frac{2x_{T_i}}{(x_{T_i}^2 + (y_{T_i}+1)^2)^{1/2}(x_{T_i}^2 + (y_{T_i}-1)^2)^{1/2}}$$

and then

$$\cot\lambda_i = \frac{x_{T_i}^2 + y_{T_i}^2 - 1}{2x_{T_i}}.$$

We note that

$$x_{T_i} - \cot\lambda_i = \frac{x_{T_i}^2 - y_{T_i}^2 + 1}{2x_{T_i}}.$$

In addition, observe that

$$\frac{\partial g_i}{\partial x_{T_i}} y_{T_i} + \frac{\partial g_i}{\partial y_{T_i}}(-x_{T_i} + \cot\lambda_i) = 0.$$

Any nullvector for the first three rows of the Jacobian matrix has the form:

$$v = [\alpha_1 y_{T_1}, \alpha_1(-x_{T_1} + \cot\lambda_1), \alpha_2 y_{T_2}, \alpha_2(-x_{T_2} + \cot\lambda_2), \alpha_3 y_{T_3}, \alpha_3(-x_{T_3} + \cot\lambda_3)]^\top$$

where the α_is are arbitrary multipliers. In order that v be a nullvector for the last three rows, it must be constructable as a linear combination of a rotation and two translations, i.e., $v_1 = [1,0,1,0,1,0]^\top$, and $v_2 = [0,1,0,1,0,1]^\top$, and $v_3 = [y_{T_1}, -x_{T_1}, y_{T_2}, -x_{T_2}, y_{T_3}, -x_{T_3}]^\top$. Hence it is desirable to investigate the solutions to the following system of equations where a, b, c, α_1, α_2, and α_3 are unknowns:

$$\begin{aligned} av_1 + bv_2 + cv_3 - v &= 0 \\ A[a,b,c,\alpha_1,\alpha_2,\alpha_3]^\top &= 0 \end{aligned} \tag{26}$$

where

$$\mathrm{A} = \begin{bmatrix} 1 & 0 & y_{T_1} & -y_{T_1} & 0 & 0 \\ 0 & 1 & -x_{T_1} & x_{T_1} - \cot\lambda_1 & 0 & 0 \\ 1 & 0 & y_{T_2} & 0 & -y_{T_2} & 0 \\ 0 & 1 & -x_{T_2} & 0 & x_{T_2} - \cot\lambda_2 & 0 \\ 1 & 0 & y_{T_3} & 0 & 0 & -y_{T_3} \\ 0 & 1 & -x_{T_3} & 0 & 0 & x_{T_3} - \cot\lambda_3 \end{bmatrix}.$$

Note that if this system of equations (26) has non-zero solutions then J_F is singular. In other words, J_F is singular if and only if A is singular. Adding the fourth, fifth, and sixth columns of A to the third one, we have

$$\mathrm{B} = \begin{bmatrix} 1 & 0 & 0 & -y_{T_1} & 0 & 0 \\ 0 & 1 & -\cot\lambda_1 & x_{T_1} - \cot\lambda_1 & 0 & 0 \\ 1 & 0 & 0 & 0 & -y_{T_2} & 0 \\ 0 & 1 & -\cot\lambda_2 & 0 & x_{T_2} - \cot\lambda_2 & 0 \\ 1 & 0 & 0 & 0 & 0 & -y_{T_3} \\ 0 & 1 & -\cot\lambda_3 & 0 & 0 & x_{T_3} - \cot\lambda_3 \end{bmatrix}.$$

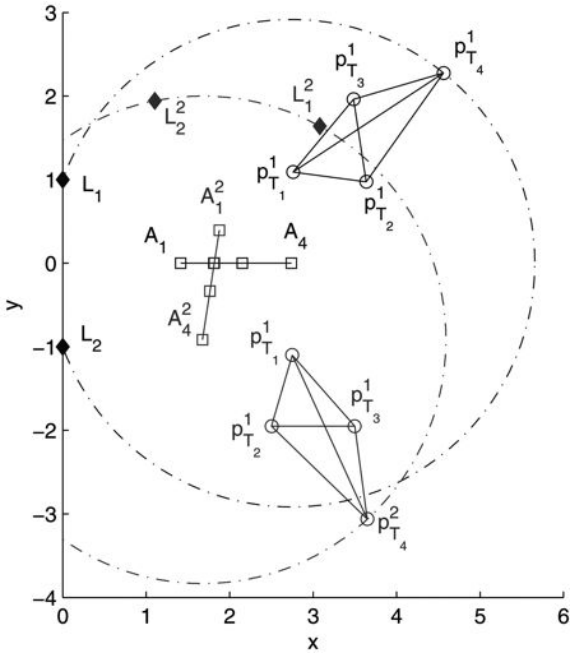

Fig. 12. Illustrative instantiation of proof of Theorem 6.

By considering the last 3 columns, that are linearly independent for generic values of angles, we see that any left nullvector of B will be of the form $u = [\alpha_1(x_{T_1} - \cot\lambda_1, \alpha_1 y_{T_1}, \alpha_2(x_{T_2} - \cot\lambda_2), \alpha_2 y_{T_2}, \alpha_3(x_{T_3} - \cot\lambda_3), \alpha_3 y_{T_3}]$. Considering the first three columns u is the left nullvector of B (and consequently A) if the system

$$\sum_{i=1}^{n}(x_{T_i} - \cot\lambda_i)\alpha_i = 0$$

$$\sum_{i=1}^{n} y_{T_i}\alpha_i = 0$$

$$\sum_{i=1}^{n} \cot\lambda_i y_{T_i}\alpha_i = 0$$

has non-zero solutions for α_i, which is equivalent to satisfying (16).

APPENDIX III. SUM OF SQUARES RELAXATION

In what follows we briefly describe how to minimize the polynomial cost functions introduced here and find their global minimizers using SOS relaxation. The full description of the method used here to find the solutions is beyond the scope of this paper and can be found in [36]–[39].

A polynomial function $f(\mathbf{x})$, $\mathbf{x} = [x_1,\ldots,x_n]$, of degree $2d$ over the polynomial ring $\mathbb{R}[\mathbf{x}]$ is SOS if one can write

$$f(\mathbf{x}) = \sum_{i=1}^{q} Q_i^2(\mathbf{x}) \tag{27}$$

where $q \in \mathbb{N}$ and $Q_i(\mathbf{x})$ are polynomials over $\mathbb{R}[\mathbf{x}]$. Denote the global minimizer and global minimum of the polynomial function $f(\mathbf{x})$, respectively, by x^* and

$\gamma = f(\mathbf{x}^*)$. x^* can be calculated solving the following optimization problem:

$$\begin{aligned} &\text{maximize} \quad \gamma \\ &\text{subject to} \quad f(\mathbf{x}) - \gamma \geq 0. \end{aligned} \tag{28}$$

One can relax (28) and write it as

$$\begin{aligned} &\text{maximize} \quad \gamma \\ &\text{subject to} \quad f(\mathbf{x}) - \gamma \quad \text{is SOS}. \end{aligned} \tag{29}$$

REMARK 6 The relaxed problem is often computationally much easier to solve, see below, and may yield the same solution. However, in general (28) and (29) are not identical, since there are positive polynomials that are not in the SOS form. For more information see [36].

It is standard that any SOS polynomial $f(\mathbf{x})$ of degree $2d$, with x an n-tuple of variables, can be written as $f(\mathbf{x}) = Z^\top WZ$, where Z is a vector of all monomials of degree up to d obtained from the variables in $\mathbf{x}$ with the first entry equal to one, and W is a positive semi-definite matrix obtained by solving a set of linear matrix inequalities (LMI) [36]. So one can reformulate (29) as,

$$\begin{aligned} &\text{maximize} \quad \gamma \\ &\text{subject to} \quad W - \hat{E}\gamma \geq 0 \end{aligned} \tag{30}$$

where $\hat{E}$ is a matrix with $E_{11} = 1$ and the rest of the entries are zero. The problem stated in (30) is a semi-definite programming (SDP) problem and can be solved by SDP techniques [36]. By solving the dual problem of the SDP problem stated in (30), one can obtain the minimizer of f as well, using the procedure in [38]. To minimize the cost functions P and P' and finding their global minimizers p_T^* and p^* in (19) and (25), we take f (and its global minimizer $\mathbf{x}^*$) to be P (and p_T^*) and P' (and p^*), respectively. In addition, we consider the following constraint optimization problem with polynomial f and h:

$$\begin{aligned} &\text{minimize} \quad f(\mathbf{x}) \\ &\text{subject to} \quad h(\mathbf{x}) = 0. \end{aligned} \tag{31}$$

Assume there exists a polynomial $\delta(\mathbf{x})$ such that

$$f(\mathbf{x}) - \gamma = \delta(\mathbf{x})h(\mathbf{x}). \tag{32}$$

Then γ is a lower bound for (31) [40]. So by maximizing γ as before one can get a lower bound that gets tighter as the degree of $\delta(\mathbf{x})$ in (32) increases. There are well-known solution procedures based on SDP iterations indicating how to choose $\delta(\mathbf{x})$ to the aforementioned problem. For more information one may refer to [36], [37], [38], [39] and references therein.

1) *Comments on the Complexity of SOS Methods*: With addition of more agents (hence introduction of more variables and consequently higher dimension LMIs) the complexity of the SOS-based solution increases rapidly but it still remains reasonable for up to 10 agents (20 variables). However, if one is interested in solving problems with a large number of variables, one should take advantage of the sparsity in the cost fucntion to reduce the size of the underlying LMIs; see [41].

To reduce the numerical sensitivity of the methods, one may want to decrease the condition number of the matrices involved in solving the optimization problems; one way to do this is to normalize the coefficients of the cost functions. The choice of the polynomial δ in (32) does not follow any rigid guidelines, but as a rule of thumb the higher order one chooses for δ the better the bound one obtains on the optimal answer, but at the expense of a considerable increase of the problem size (i.e., increase in matrix dimensions).

REFERENCES

[1] Ward, P. W.
GPS receiver RF interference monitoring, mitigation and analysis techniques.
Navigation, **41** (Winter 1995–1994), 367–391.

[2] Dedes, G. and Dempste, A. G.
Indoor GPS positioning: Challenges and opportunities.
In *Proceedings of the IEEE Conference on Vehicular Technology*, Dallas, TX, Sept. 2005, 412–415.

[3] Carroll, J. V.
Vulnerability assessment of the US transportation infrastructure that relies on the Global Positioning System.
The Journal of Navigation, **56** (2003), 185–193.

[4] Betke, M. and Gurvits, L.
Mobile robot localization using landmarks.
IEEE Transactions on Robotics and Automation, **13** (1997), 251–263.

[5] Shimshoni, I.
On mobile robot localization from landmark bearings.
IEEE Transactions on Robotics and Automation, **13** (2002), 971–976.

[6] Hmam, H.
Mobile platform self-localisation.
In *Proceedings of Information Decision and Control*, Adelaide, Australia, Feb. 2007, 242–247.

[7] Jesteves, J. S., Carvalho, A., and Couto, C.
Generalized geometric triangulation algorithm for mobile robot absolute self-localization.
In *Proceedings of the IEEE International Symposium on Industrial Electronics*, Rio de Janeiro, Brazil, June 2003, 346–351.

[8] Ryde, J. and Hu, H.
Fast circular landmark detection for cooperative localisation and mapping.
In *Proceedings of the International Conference on Robotics and Automation*, Barcelona, Spain, Apr. 2005, 2745–2750.

[9] Bishop, A. N., et al.
Bearing-only localization using geometrically constrained optimization.
IEEE Transactions on Aerospace and Electronic Systems, **45** (2009), 308–320.

[10] Taff, L. G.
Target localization from bearings-only observations.
IEEE Transactions on Aerospace and Electronic Systems, **33**, 1 (1997), 2–10.

[11] Eren, T., et al.
Rigidity, computation and randomization in network localization.
In *Proceedings of Network Localization, Joint Conference of IEEE Computer and Communication Societies*, Hong Kong, Mar. 2004, 2673–2684.

[12] Roumeliotis. S. I. and Bekey, G. A.
Collective localization: A distributed Kalman filter approach to localization of groups of mobile robots.
In *Proceedings of International Conference on Robotics and Automation*, San Francisco, CA, Apr. 2000, 2958–2965.

[13] Kwok, N. M., Dissanayake, G., and Ha, Q. P.
Bearing-only SLAM using a SPRT-based Gaussian sum filter.
In *Proceedings of International Conference on Robotics and Automation*, Barcelona, Spain, Apr. 2005, 1109–1114.

[14] Laman, G.
On graphs and rigidity of plane skeletal structures.
Journal of Engineering Mathematics, **11** (1970), 331–340.

[15] Tay, T. and Whiteley, T.
Generating isostatic frameworks.
Structural Topology, **11** (1985), 21–69.

[16] Anderson, B. D. O., et al.
Rigid graph control architectures for autonomous formations.
IEEE Control Systems Magazine, **28** (2008), 48–63.

[17] Yu, C., et al.
Merging multiple formations: A meta-formation prospective.
In *Proceedings of Conference on Decision and Control* (CDC 2006), San Diego, CA, Dec. 2006, 4657–4663.

[18] Mao, G., Fidan, B., and Anderson, B. D. O.
Localization.
In *Sensor Networks and Configuration: Fundamentals, Techniques, Platforms and Experiments*, New York: Springer-Verlag, 2006, ch. 13, 281–315.

[19] Hendrickson, B.
Conditions for graph unique realizations.
SIAM Journal on Computing, **21** (1992), 65–84.

[20] Jackson, B. and Jordan, T.
Connected rigidity matroids and unique realizations of graphs.
Journal of Combinatorial Theory Series B, **94** (2005), 1–29.

[21] Beyer, R.
Kinematic Synthesis of Mechanisms.
(Translated from German by H. Kuenzel), London: Chapman and Hall, 1963.

[22] Chung, W.
The characteristics of a coupler curve.
Mechanism and Machine Theory, **40**, 10 (2005), 1099–1106.

[23] Yu, G. and Yu, F.
A localization algorithm for mobile wireless sensor networks.
In *Proceedings of the 2007 IEEE International Conference on Integration Technology*, Shenzhen, China, Mar. 2007, 623–627.

[24] Zhou, X. S. and Roumeliotis, S. I.
Determining the robot-to-robot relative pose using range-only measurements.
In *Proceedings of the International Conference on Robotics and Automation*, Rome, Italy, Apr. 2007, 4025–4031.

[25] Zhou, X. S. and Roumeliotis, S. I.
Robot-to-robot relative pose estimation from range measurements.
IEEE Transactions on Robotics, **24**, 6 (2008), 1379–1393.

[26] Piovan, G., et al.
On frame and orientation localization for relative sensing networks.
Center for Control, Dynamical Systems and Computation, University of California at Santa Barbara, Technical Report, 2008.

[27] Piovan, G., et al.
On frame and orientation localization for relative sensing networks.
In *Proceedings of the 47th IEEE Conference on Decision and Control*, Cancun, Mexico, Dec. 2008, 2326–2331.

[28] Shames, I., et al.
Self-localization of mobile agents in the plane.
In *Proceedings of the International Symposium on Wireless Pervasive Computing*, Santorini, Greece, May 2008, 116–120.

[29] Tutte, W. T.
A theory of 3-connected graphs.
Indagationes Mathematicae, **23** (1961), 441–455.

[30] Yu, C., Fidan, B., and Anderson, B. D. O.
Principles to control autonomous formation merging.
In *Proceedings of American Control Conference*, Minneapolis, MN, June 2006, 762–768.

[31] Yarlagadda, R., et al.
GPS GDOP metric.
IEE Proceedings, Radar, Sonar and Navigation, **147**, 5 (Oct. 2000), 259–264.

[32] EPFL education robot
http://www.e-puck.org/.

[33] Siegwart, R. and Nourbakhsh, I. R.
Introduction to Autonomous Mobile Robots.
Cambridge, MA: MIT Press, 2004.

[34] Cao, M., Anderson, B. D. O., and Morse, A. S.
Sensor network localization with imprecise distances.
Systems and Control Letters, **55** (Nov. 200), 887–893.

[35] Shames, I., et al.
Polynomial methods in noisy network localization.
In *Proceedings of Mediterranean Control Conference*, June 2009.

[36] Parrilo, P.
Semidefinite programming relaxations for semialgebraic problems.
Mathematical Programming, **96**, 2 (2003), 293–320.

[37] Parrilo, P. A. and Sturmfels, B.
Minimizing polynomial functions.
DIMACS Series in Discrete Mathematics and Theoretical Computer Science, vol. 60, 2003, 83–99.

[38] Henrion, D. and Lasserre, J.
Detecting global optimality and extracting solutions in GloptiPoly.
In D. Henrion and A. Garulli (Eds.), *Positive Polynomials in Control*, Lecture Notes on Control and Information Sciences, New York: Springer-Verlag, 2005.

[39] Lasserre, J.
Global optimization with polynomials and the problem of moments.
SIAM Journal on Optimization, **11** (2001), 796–817.

[40] Schmudgen, K.
The K-moment problem for compact semi-algebraic sets.
Mathematische Annalen, **289**, 1 (1991), 203–206.

[41] Nie, J., Demmel, J., and Sturmfels, B.
Minimizing polynomials via sum of squares over the gradient ideal.
Mathematical Programming, **106**, 3 (2006), 587–606.

Iman Shames received his B.S. degree in electrical engineering from Shiraz University, Iran in 2006. He is a NICTA-endorsed Ph.D. candidate at the Australian National University, Canberra, Australia, under the supervision of Prof. Brian D. O. Anderson, and holds an EIPRS (Endeavour International Postgraduate Research Scholarship).

He was a visiting researcher at the Royal Institute of Technology (KTH) in 2009 and 2010, the University of Tokyo in 2008, and at the University of Newcastle in 2005. His current research interests include multi-agent systems, sensor networks, systems biology and distributed fault detection and isolation.

Barş Fidan received the B.S. degree in electrical engineering and mathematics from Middle East Technical University, Turkey in 1996, the M.S. degree in electrical engineering from Bilkent University, Turkey in 1998, and the Ph.D. degree in electrical engineering at the University of Southern California, Los Angeles, in 2003.

He worked at the University of Southern California in 2004 as a postdoctoral research fellow, and at the National ICT Australia and the Research School of Information Sciences and Engineering of the Australian National University in 2005–2009 as researcher/senior researcher. He is currently an assistant professor at the Mechanical and Mechatronics Engineering Department, University of Waterloo, Canada. His research interests include autonomous multi-agent dynamical systems, sensor networks, cooperative localization, adaptive and nonlinear control, switching and hybrid systems, mechatronics, and various control applications including high performance and hypersonic flight control, semiconductor manufacturing process control, and disk-drive servo systems.

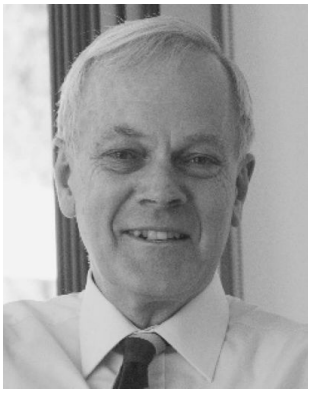

Brian D. O. Anderson (M'66—SM'74—F'75—LF'07) was born in Sydney, Australia, and educated at Sydney University in mathematics and electrical engineering, with a Ph.D. in electrical engineering from Stanford University, Stanford, CA, in 1966.

He is a distinguished professor at the Australian National University and Distinguished Researcher in National ICT Australia. His current research interests are in decentralized control, sensor networks and econometric modelling.

Dr. Anderson's awards include the IEEE Control Systems Award of 1997, the 2001 IEEE James H. Mulligan, Jr. Education Medal, and the Bode Prize of the IEEE Control System Society in 1992.

Hatem Hmam received his Ph.D. degree in electrical engineering from University of Cincinnati, Cincinnati, OH, in 1992.

He pursued post-doctoral research in jet engine control at the University of Colorado, Boulder, and signal processing at Queensland University of Technology, Brisbane, Australia, before joining the Defence Science and Technology Organisation in 1996. He is currently working on electronic warfare projects. His research interests include passive emitter localization.